Document for	SAC/STAP evaluation
Project Name	MAGiC
Date	Apr 16, 15, 7:28 AM

ESS Instrument Construction Proposal

MAGnetIC single crystal diffractometer

MAGiC

	Name	Affiliation
Proposers	Xavier Fabrèges Arsen Goukassov	Laboratoire Léon Brillouin CEA Saclay 91191 Gif sur Yvette, France
	Michel Kenzelmann	Paul Scherrer Institut, Villigen, Switzerland
	Werner Schweika	ESSS, Lund, Sweden
Co-proposers	Yixi Su, Jörg Voigt, Earl Babcock	JCNS, Forschungszentrum Jülich, Germany
	Uwe Filges	Paul Scherrer Institut, Villigen, Switzerland
	Andrew Sazonov	Technical University of Aachen
	Beatrice Gillon, Alexandre Bataille, Isabelle Mirebeau, Philippe Bourges, Yvan Sidis	Laboratoire Léon Brillouin CEA Saclay 91191 Gif sur Yvette, France
	Fabienne Duc, Paul Frings	LNCMI-Toulouse, France
	Virginie Simonet	Institut Néel, CNRS Grenoble, France
	Josep Nogués Sanmiquel	Univ. Autonoma Barcelona, Spain
	Jose Luis Garcia-Munõz	ICMAB-SIC, Barcelona, Spain
	Igor Golosovsky	PNPI, Kurchatov Institut, Gatchina, Russia
ESS coordinator	Werner Schweika	

The following table will be used only for the final submission of the proposal to the SAC. (Distribution now shown in black)

	Name
Document submitted to	Ken Andersen
Distribution	Dimitri Argyriou, Oliver Kirstein, Arno Hiess, Robert Connatser, Sindra Petersson Årsköld, Richard Hall-Wilton, Phillip Bentley, Iain Sutton, Thomas Gahl, relevant STAP

European Spallation Source ESS AB
Visiting address: ESS, Tunavägen 24
P.O. Box 176
SE-221 00 Lund
SWEDEN

www.esss.se

Executive Summary

Magnetism plays a crucial role in our modern societies. The use of magnetism is widespread and can be found in the strategically important industries, such as energy, health, transport and information technology. In the energy sector, magnetism is used to generate electricity from renewable energy sources such as hydropower and wind. In the health industry, magnetic resonance imaging (MRI) is now an established advanced imaging technique and has revolutionized the way that human health can be monitored. In the transport industry, permanent magnets transform electric energy into motion and thus are decisive in our quest for cleaner cars and trucks. In information technology, magnetism is an important technique for the storage of digital information.

Many of the recent applications of magnetism are a result of fundamental research, some of which have occurred only in the last 30 to 40 years, including the development of the permanent $Nd_2Fe_{14}B$ magnets in the 1980ies and the study of the giant magneto resistance effect in the 1990ies. MRI was a side product of a pure academic research of nuclear magnetic resonance in the last 50 years. These are only a few examples that illustrate how important magnetism has been and continues to be for our technological progress.

Neutron diffraction is the most powerful technique to quantitatively study magnetic properties on an atomic scale. Magnetic neutron diffraction takes advantage of the neutron magnetic moment and gives a direct access to the spin and orbital distribution in the unit cell. The method is widely used by the condensed matter physics, chemistry, material science and engineering. Neutron diffraction is particularly powerful when used with polarized neutrons.

In the last 50 years, an increasing number of materials have been discovered that show novel physical properties that are only partially understood. In a large fraction of these materials, the electronic states that give rise to the novel physical properties involve spin or orbital degree of freedom, which is also the origin of magnetism. Examples can be found in diverse areas, some of which could have technological applications in the medium term. This includes novel forms of superconductivity and ferroelectricity – materials properties that are widely used in industry, and where novel materials could lead to an increase in energy efficiency or to an enhanced performance. Other materials feature novel states at low temperatures, such as spin liquids or complex magnetic structures with emergent properties, which may have applications in the long term.

The understanding of magnetic structures is crucial for our understanding of such novel phenomena. The properties of magnetic structures, including their symmetries, determine how magnetism can couple to the atomic lattice or to charge degrees of freedom. Magnetic neutron diffraction is the leading and unbeaten experimental method to study magnetic structures and provides information that cannot be obtained by any other method, including magnetic X-ray diffraction. Particularly useful in this respect is magnetic neutron diffraction from single-crystals because of its higher sensitivity to small magnetic signals.

Of high current interest in the scientific community is the role of spin-orbit interactions in solid materials and complex magnetic structures arising from competing interactions. Examples of current hot topics include the physical properties of iridium oxide materials, novel spin textures found in skyrmion-featuring materials, the complex interplay of magnetism and superconductivity in unconventional superconductors (pnictidies, cuprates, heavy-fermion intermetallics and organic superconductors), multifunctionality in magnetically-induced ferroelectrics, and frustrated or low-dimensional magnetic materials featuring strong

magnetic correlations or spin-liquid-like quantum coherent ground states. Some of these materials cannot be studied at present due to the lack of large enough single-crystalline materials.

The importance of magnetic neutron diffraction for the condensed matter science community is reflected in the publication record. According to Web of Science, there are about 100 annual publication for the search: neutron AND magnetic AND "single crystal" AND diffraction. This underlines the importance of magnetic neutron diffraction from single crystals.

We propose to build a novel high-performing MAGnetiC single-crystal diffractometer (MAGiC) that is dedicated to magnetic structure determination using small single-crystalline samples. It will complement other ESS instruments which allow the study of magnetic properties in solid matter, such as the SANS, reflectometry, powder diffraction and chopper spectrometer. Single crystal diffraction using *neutron time-of-flight Laue technique* will most strongly profit from the long pulse structure of the ESS, as already shown for macromolecular crystallography. The combination of the Laue technique with the exceptional brilliance of the ESS thermal and cold moderators yields gains of about two orders of magnitude or more compared to currently existing instruments.

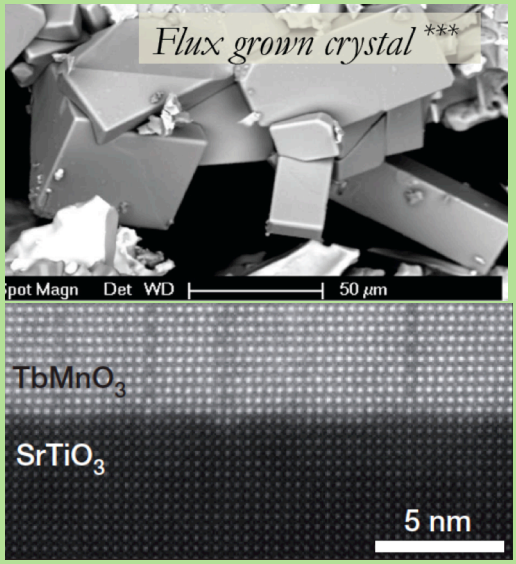

Figure 1: (top): Many materials can only be synthesizes as very small single crystals (courtesy Dr. M. Valldor). (bottom): The combination of materials can lead to technologically important properties, such as novel magneto-electric coupling [S. Farokhipoor et al, Nature Materials **515**, 379 (2015)].

In order to take full advantage of the polarized neutron cross-section, the incident beam will be fully polarized in both the cold and thermal energy range. The ESS instrument MAGiC will offer the most intense polarized neutron beam. This opens up completely new perspectives in magnetic neutron diffraction. Sample volumes that are smaller by 2-3 orders of magnitude than currently used can be measured without the need to carefully align single-crystals beforehand. Special care will be taken to reduce the instrument background as much as possible.

The proposed instrument will be optimized for small samples. This is important for two reasons: firstly, many novel materials can only be made in small single crystals, and can thus not be studied at present using magnetic single-crystal diffraction. Secondly, MAGiC will be equipped with complex sample environment including high-pressure cells, sub-Kelvin low-temperature cyrostats and state-of-the-art superconducting magnets (providing field in excess of 20T), where the sample volume is limited. An optimized diffractometer for small single-crystals will allow taking full advantage of both the technological advance in neutron and sample environment instrumentation. The instrument will provide a large area detector and a complementary detector with smaller vertical aperture dedicated to polarization analysis by supermirrors. Comparison of MAGiC with the best known current instrumentation shows impressive gains also in unpolarized neutron flux, as well as much more efficient 3D Q-space sampling with better resolution.

The maturity of this ESS instrument proposal in view of construction is supported by i) the use of existing state-of-the art technology and ii), the expertise of the institutes: LLB leading the instrument construction (single crystal magnetic structure determination), supported by PSI (neutron optics, supermirror technology) and JCNS (diffuse scattering and polarization analysis, ^{3}He polarization).

Table of contents

1. Scientific Case

Magnetism is ubiquitous in our modern societies. We rely heavily on magnetic properties of devices and materials. The measurement of macroscopic magnetic properties is widely available, and can be performed to high accuracy with superconducting quantum interference devices (SQUID). The measurement of microscopic magnetic properties is less widely available, and many techniques have severe limitations. Nuclear magnetic resonance (NMR) and muon spin spectroscopy (muSR) are popular techniques to study microscopic magnetic properties, but they rely on local magnetic probes and can thus not determine the nature of the magnetic order in many materials. Magnetic X-ray scattering is in principle able to detect long-range magnetic order, but the wave-vector accessibility is limited and does not allow a quantitative determination of magnetic structures. Magnetic neutron diffraction is currently the only technique that can provide both the symmetry of a magnetic structure and a quantitatively determination of the ordered magnetic moment.

Figure 2: Many of todays electric motors depend on high energy density permanent magnets: Loadstone, ferrite and NdFeB magnet: each stores the same magnetic energy (~0.4J), yet the mass has decreased a thousand fold [R. Harris & A.J. Williams, Materials World **7**, 478 (1999)].

It is therefore no surprise that magnetic neutron diffraction on single-crystals is a widely used technique to study the microscopic magnetic properties of solid materials. The illustrious history dates back to Shull's [1] discovery of magnetic Bragg peaks in MnO in 1949 that had been predicted by Néel. Since these early studies, magnetic neutron diffraction and its analysis has made several important advances: on the analysis side the most important development was probably the theory of irreducible representations [2] and co-representations [3] for describing magnetic structures, the publication of several programs that calculate the basis vectors of magnetic structures[4]. Also important is the availability of refinement code for single-crystal magnetic diffraction data[5].

In the early days of neutron scattering, experiments were limited by both the scattering intensity and the refinement techniques. The focus was on the determination of the main features of magnetic structures, or on materials having relatively simple magnetic structures. The need for more advanced techniques to determine magnetic structures became apparent with the advent of unconventional superconductivity and frustrated magnetism from the mid 1980ies onwards. Such materials either feature magnetic structures with tiny magnetic moments, which were difficult to detect, or the structures are complex and involve several irreducible representations (several types of symmetries).

Magnetism can have an important effect on other physical properties of materials, for example electric and transport properties. The coupling of magnetism with physical properties was heavily studied in the superconducting cuprates and other unconventional superconductors, and materials featuring colossal magneto-resistance (CMR) where a change in magnetization leads to a "colossal" change in resistance

[1] C.G. Shull and J. Smart, Phys. Rev. B **76**, 1256 (1949).
[2] E.F. Bertaut, Acta Cryst. **A24**, 217 (1968).
[3] J. Schweizer, C.R. Physique **6,** 375 (2005).
[4] MODY, BASIREPS, Sarah
[5] J. Rodriguez-Carvajal, Physica B **192**, 55 (1993).

involving double-exchange of electrons.[6] Complex magnetic structures are often observed in the vicinity of novel quantum phases or in the presence of competing interactions. Complex magnetic structures can yield novel behavior, such as magnetically-induced ferroelectricity in insulators[7], spontaneous Hall effects in metals[8], novel Mott insulator transitions[9] and long-wave-length spin textures in skyrmion materials[10]. Spin-orbit interactions often play an important role in these phenomena.

Today, many novel materials cannot be studied with neutron diffraction, either because the magnetic moments are small, or because the samples are too small. Both effects lead to small magnetic Bragg peak intensities, which can make it impossible to even observe a single magnetic Bragg peak in many materials. With the increased flux at ESS, new concepts for neutron guides and advanced simulation techniques to estimate the background, we are now in the position to significantly extend the use of magnetic neutron diffraction to sample volumes of 10^{-3} mm^{-3}, which are 2-3 orders of magnitude smaller than currently possible. The higher efficiency will make it possible to study transition metal-oxide thin films and heterostructures using magnetic neutron diffraction on a routine basis – experiments that are currently at the forefront of experimental physics.

The use of analysis software today is restricted to a small circle of experts. The requirement for relatively large single crystals additionally restricts the use of single-crystal magnetic neutron diffraction. This greatly limits the impact of magnetic neutron diffraction from single crystals in the condensed matter and materials science communities. MAGiC will accept small single-crystals, that do not have to be aligned as carefully as on current neutron diffractometers. This will greatly reduce the barrier to entry for new neutron users, particularly if it is also supported by advances in analysis software. The improvement in the data collection speed together with analysis software will make magnetic neutron diffraction accessible to a much wider community of non-experts.

We will now describe a series of scientific areas, which we think will particularly strongly benefit from MAGiC. The main areas include 1) materials in which magnetic structures, or short-range correlations, are coupled with the mobile charge carriers, leading to metal-insulator transitions, 2) unconventional superconductors in proximity of magnetic phases, 3) materials with strong magnetic fluctuations and (quantum) phase transitions into novel magnetic phases, 4) magnetic insulators with a strong coupling to the atomic lattice, leading to ferroelectricity or other types of electric phenomena, 5) metals where strong spin fluctuations lead to anisotropic transport phenomena and charge/spin Hall effects, and finally 6) physics in thin films and heterostructures.

Magnetism and metal-insulator transitions

A particularly interesting area is the interplay between magnetism and transport properties. A simple case is a metal that develops ferromagnetic order, such as metallic Fe or many of the ferrites, which have partly filled electron bands. The presence of spontaneous ferromagnetism is associated with an unequal population of the electron bands for spin up and spin down. However, the materials still function essentially like basic metals where electrons behave as particles with a weak effective interaction with other electrons in the Fermi sea.

[6] A.P. Ramirez, J. Phys.: Condens. Matter **9**, 8171 (1997).
[7] T. Kimura et al, Nature **426**, 55 (2003).
[8] Y. Machida et al, Nature **463**, 210 (2010).
[9] B.J. Kim et al, Phys. Rev. Lett. **101**, 076402 (2008).
[10] S. Mühlbauer et al, Science **323**, 915 (2009).

Strong electron-electron interactions fundamentally change this scenario. An illustrative model is the single-band Hubbard model, in which the electrons can hop from one site to the next with frequency τ, and an energy U has to be paid if two electrons populate the same site. At half filling and for U=0, this stabilizes a metallic state, but for sufficiently large U, an insulating state is obtained.. This insulating state is called a Mott insulator and illustrates how strong electron-electron interactions, including magnetic properties, can fundamentally change the transport properties of a material. It was recently shown in the now famous iridates that strong spin-orbit interactions lead, in a different way, to Mott-like insulating states from half-filled electron bands.[11] Another scenario is a charge-transfer between ions that change the single-ion properties such as the moment formation on a single ion.

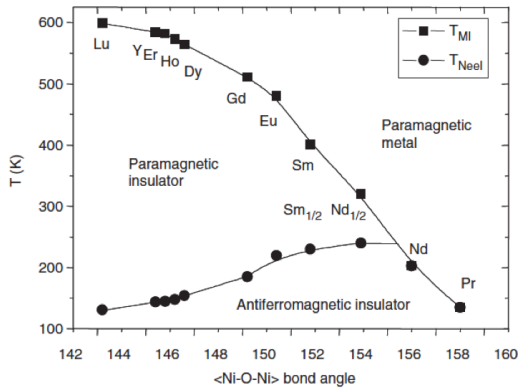

Figure 3: Phase diagram of $RNiO_3$ as a function of the Ni-O-Ni bond angle and temperature: the magnetic and metal-insulator transition is identical for $NdNiO_3$ and $PrNiO_3$ [G. Catalan, Phase Transitions **81**, 729 (2008)].

Real materials introduce additional degrees of freedom. For example, several degenerate orbitals or bands can be responsible for the transport properties that can lead to spontaneous order of orbital states. Such phenomena can be associated with Jahn-Teller distortions, or disproportionation of charge into spontaneously charge-ordered states that are a direct result of strong electron-electron interactions.

There are several material classes where the effect of strong electron-electron interactions on the transport can be studied. In the presence of unpaired electron in orbitals of transition metal ions, the magnetic properties are intricately linked to the transport properties. The study of such phenomena enormously profits from the use of neutron diffraction. However, many of the interesting materials can only be made in small quantities, and have thus not been studied using neutron diffraction.

One such example is the rare-earth (R) nickelate series, $RNiO_3$, which features a metal-insulator transition that is partly coupled with onset of magnetic order.[12] These materials are metallic at high temperatures, and develop a semiconducting ground state below T=400K, with the exception of $LaNiO_3$ (see Figure 3). For small rare-earth radii, antiferromagnetic order appears in the insulating phase. With increasing rare-earth radius, the metal-insulator and magnetic phase transitions occur at the same temperature, demonstrating the strong coupling between magnetic and transport properties. The mechanism that leads to the metal-insulator transition is poorly understood. It has also been suggested that multiferroicity appears in the antiferromagnetic phase, which is another indication of a strong coupling between charge and magnetic degrees of freedom. Advances in single-crystal growth under high oxygen pressure will likely make it possible to produce small single-crystals of these materials. MAGiC will be ideally suited to study single-crystalline magnetic properties as a function of magnetic field and high pressure.

[11] B.J. Kim et al, Phys. Rev. Lett. **101**, 076402 (2008).
[12] M. Medarde et al, J. Cond. Matt. Phys. **9**, 1679 (1996).

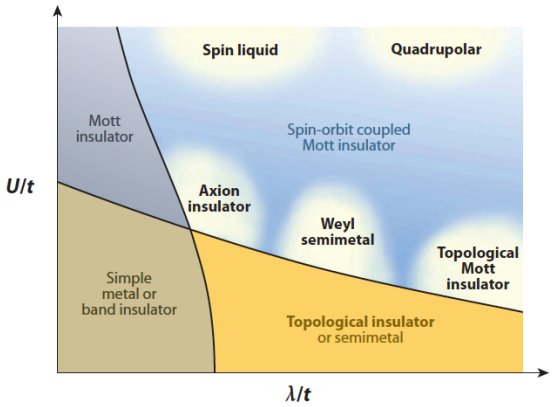

Figure 4: A generic phase diagram *vs* on-site Coulomb interaction (U/t) and spin-orbit coupling (λ/t) in iridates.[14]

The size of suitable samples has also been a great obstacle of the magnetic properties of many iridium oxides, which can only be synthesized as very small crystals. This is an important field with the potential to make textbook experiments to study the magnetism of novel Mott-like insulating states. Single-crystal diffraction is an important tool to determine the symmetry of magnetism and quantify the magnetic moments. A polarized single crystal diffractometer optimized for small samples will be ideal for such experiments. Cold polarized neutrons can be used to collect large data sets to determine the magnetic structure. Thermal polarized neutrons with a magnetic field can be used to perform magnetic form factor measurements for each individual material. Such measurements will provide accurate information about the form factor when strong covalency effects are present. This will be important to quantify not only the ordered magnetic moment, but also for inelastic scattering experiments measured on the same samples using the chopper spectrometers at ESS. This can be a crucial aspect, as a study on Sr_2CuO_3 has shown: only a determination of the form factor allowed for a quantitative understanding of the magnetism involved in the magnetic correlations and solved a long-standing enigma.[13]

Novel topological states can also emerge in the strongly correlated magnetic Coulomb phase when the spin-orbit entanglement is combined with electronic Coulomb interaction, as shown in Fig. 4.[14] In particular, such quantum spin liquid and quadrupolar ordered phases have been suggested to occur in iridates and double perovskites. These would arise from multipolar interactions, which promote strong quantum fluctuations. Applying a magnetic field can reveal the underlying antiferromagnetic quadrupolar order through the appearance of field-induced antiferromagnetic reflections.[15]

Magnetism and superconductivity

Conventional *s*-wave superconductors feature an attractive phonon-mediated force between two electrons, which leads to the formation of Cooper pairs. Cooper pairs consist of two fermions and are bosons that can condense into macroscopic quantum state that is superfluid, has no resistance and expels magnetic fields: superconductivity. A theory developed by Bardeen, Cooper and Schrieffer (BCS) explains many of the characteristic features of conventional superconductors, and established a competition between magnetism and superconductivity.

In 1979, Steglich observed that $CeCu_2Si_2$ becomes superconducting in the presence of strong magnetic fluctuations, which was in contradiction to BCS theory.[16] In the following years, a number of so-called heavy-fermion superconductors were discovered, highlighting the role magnetic fluctuations in the pairing mechanism. High-T_c superconductivity (HTS) was discovered in 1986,[17] and its pairing mechanism remains to be understood. It is nevertheless well accepted now that HTS is unconventional and is

[13] A.C. Walter set al, Nature Physics **5**, 867 (2009).
[14] W. Witczak-Krempa, G. Chen, Y.B. Kim and L. Balents. *Annual Review of Cond. Matter Physics* **5**, 57 (2014).
[15] M. Kohgi et al. J. Phys. Soc. Japan. Lett. **72**, 5, 1002 (2003)
[16] F. Steglich et al, Phys. Rev. Lett. **43**, 1892 (1979).
[17] J.G. Bednorz and K.A. Müller, Z. Phys. **67**, 285 (1987).

accompanied by the occurrence of an enigmatic "pseudo-gap" phase prefiguring the superconductivity state. Theoretically, valence and/or magnetic fluctuations are the key ingredients in the pairing mechanism. Experimentally a fascinating interplay between magnetism and superconductivity has been observed.

There are many open questions in the field of superconductivity, many of which can be addressed with magnetic neutron diffraction. At sub-Kelvin temperature, neutron diffraction is currently the only technique that can determine the symmetry of magnetic order. The relatively large wave-vector coverage of cold and thermal neutron diffraction makes it the only method available to quantitatively determine magnetic structure at any temperature. Polarized thermal neutron Laue diffraction allows a quantitative determination of the form factor, which reflects the hybridization of localized spin degrees of freedom with the environment, and polarized Laue diffraction will be efficient way to perform such measurements.

It is probably fair to say that **HTS** is poorly understood. For some time, the superconductivity appeared as a special case developping in the proximity of a Mott insulator upon charge coping. The magnetism in the cuprates is that of two-dimensional sheets of fairly localized magnetic moments. The discovery of the pnictides superconductors showed that a similar phase diagram is also achieved for more itinerant magnetism and larger spin. In high-T_c superconductors, different ground states compete strongly, leading to chemical phase transition in some of the pnictides, to charge ordered states or spin density wave order that compete with superconductivity, or stripe type patterns. In order to answer basic questions in these materials, and characterize their microscopic magnetic order parameter, polarized neutron diffraction plays an important role.

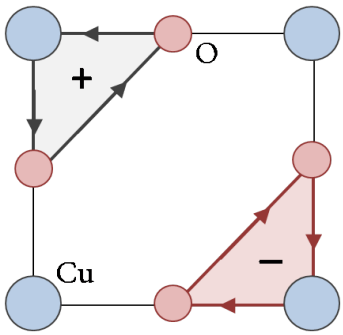

Figure 5: Predicted spontaneous orbital current distribution in the high-T_c cuprates.[18]

One important question in the high-T_c superconductivity concerns the so-called pseudo-gap phase, where an opening of in the electronic spectrum is observed at relatively high temperature. Among the scenarios that were proposed is the presence of a hidden order parameter[18] which consists of an orbital loop currents. Such pairs of closed current loops were proposed to rotate clockwise and anticlockwise in each unit-cell, producing staggered orbital magnetic moments that can be detected using neutron scattering. Search for the Varma state using neutron diffraction is extremely challenging, since the circulating current state preserves the lattice translation invariance: the expected magnetic signal is about four orders of magnitude weaker than the most intense nuclear Bragg peaks and is superimposed on the nuclear Bragg reflections. Nevertheless, polarized neutron diffraction has identified novel magnetic order in the copper oxide family $YBa_2Cu_3O_{6+x}$, occurring at the transition temperature where the pseudo-gap opens.[19] The observed magnetic order preserves translational symmetry but breaks time reversal symmetry as predicted in the loop current theory. However, only a limited number of Bragg reflections were accessible in the experiments, so neither the symmetry of the current loop order nor its form factor could be determined. Neutron diffraction measurements with much higher sensitivity covering a larger wave-vector range are needed, as it will be possible on MAGiC, to discriminate whether the magnetic Bragg peaks could also

The magnetic moment is a vector ↑ →

Usually intensities are only measures of scalar products.
The neutron dipolar interaction probes magnetic moments perpendicular to the scattering vector $\vec{S}_{\perp\vec{Q}} \cdot \vec{S}'_{\perp\vec{Q}}$

Polarized neutrons measure vector properties, vector products and vector directions $\vec{S}_{\perp\vec{Q}} \times \vec{S}'_{\perp\vec{Q}}$

[18] C.M. Varma, *Phys. Rev.* B**55** 14554 (1997); B**73** 155113 (2006). Phys. Rev. Lett. **83** 3538 (1999)
[19] B. Fauqué et al, Phys. Rev. Lett. **96** 197001 (2006), V. Balédent et al, Phys. Rev. Lett. **105** 027004 (2010)

arise from magnetic order on the oxygen sites.

An important class of superconductors that has barely been studied with neutron scattering are the **organic superconductors.**[20] These are materials that consist of large molecules, and magnetism emerges through charge transfer. Superconductivity occurs at temperatures of the order of T=10K and below. This class of materials has been strongly studied by magnetization and transport measurements, but the microscopic measurements are dominated by NMR measurements. The experimental results point towards a rich interplay between magnetism and superconductivity. Novel superconducting phases such as the Fulde-Ferrell-Larkin-Ovchinnikov phase with modulated superconductivity were reported.[21] The single-crystals are often of sub-milimeter size, and therefore too small to detect magnetic order directly with neutron diffraction with the existing instrumentation.

Together with the organic superconductors, ***f*-electron superconductors** are probably the best model materials to study many fundamental aspects of superconductivity. Strong fluctuations in *f*-electron metals can arise firstly because the f-electrons associated with rare-earth ions can be either localized or mobile, leading to strong charge fluctuations, and secondly because these materials can be in the vicinity of a magnetic quantum critical point.[22] Superconductivity appears to emerge when strong fluctuations exist down to low temperatures. These materials feature an intricate relationship between magnetism and superconductivity. One of the clearest examples in this respect may be $CeCoIn_5$, where a spin-density wave occurs inside the superconducting phase, and disappears at the upper critical fields where the material becomes a resistive conductor.[23] Such experiments can be performed today, but are extremely slow and do not allow measuring quantum critical exponents with high accuracy. In addition, there are similar layered superconductors, such as $CePt_2In_7$, which becomes superconducting under pressure and can be synthesized only as small single crystals.[24] It orders antiferro-magnetically below T = 5.2K, but its magnetic order parameters have not been studied so far due to the lack of suitable probe. A greatly improved signal-to-noise on MAGiC will allow these experiments to be taken to the next level, and provide information of magnetic quantum phase transitions in a wider range of superconductors.

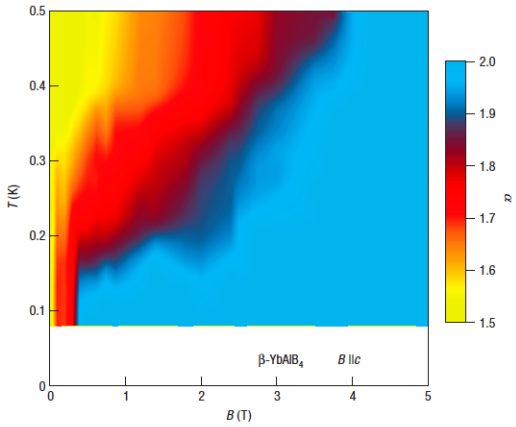

Figure 6: Temperature-field diagram of $YbAlB_4$ assembled from the temperature dependence of the resistivity (constant + $T^{\square}$), showing that α is equal to 2 in a large area part of the phase diagram, which is a sign of strong electron-electron interactions.[25]

There are other important model superconductors whose microscopic magnetic properties have not yet been determined because of the absence of large enough crystals, or insufficient scattering intensity to background. For example, $YbAlB_4$ was the first Yb heavy-fermion superconductor, and is the hole-doped equivalent of Ce-based superconductors.[25] The magnetism appears to be low-dimensional and play an important role for superconductivity. Unfortunately, it can only be made as extremely small single crystals and so the microscopic magnetic properties are largely unknown.

[20] H. Mori, J. Phys. Soc. Jpn. **75**, 051003 (2006).
[21] R. Casalbuoni and G. Ardulli, Rev. Mod. Phys. **76**, 263 (2004).
[22] C. Pfleiderer, Rev. Mod. Phys. **81**, 1551 (2009).
[23] S. Gerber et al, Nature Physics **10**, 126 (2014).
[24] E.D. Bauer et al, Phys. Rev. B 81, 180507(R) (2010).
[25] K. Kuga et al, Phys. Rev. Lett. **101**, 137004 (2008).

The study of the magnetic properties of unconventional superconductors holds great opportunities when neutron diffraction experiments become possible on small single crystalline materials. The interplay between magnetic and superconducting properties can lead in principle to many coupled order parameters and MAGiC with its focus on small samples, neutron polarization and low background will undoubtedly be able to contribute greatly to this field.

Magnetism in frustrated and quantum magnetic insulators

Magnetic order in materials close to a quantum critical point often features small magnetic moments. As a result, it has been inherently difficult to track down these crucial order parameters and measure critical exponents. Quantum critical points are strictly speaking located at zero temperature, and are driven by quantum fluctuations that are tuned with magnetic or electric fields, hydrostatic pressure or stress. The typical sample environment for the investigation of magnetic quantum critical points consist of low-temperature cryostats with a dilution refrigerator, high-field magnets and high-pressure cells. Often it is desirable to combine some of these capabilities, such as high-pressure cells cooled by a He^3 cryostat and exposed to high magnetic fields.

Some of the simplest systems to study quantum critical points are insulators with localized low-spin degrees of freedom. A good example is the S=1 antiferromagnetic chain that features a quantum spin liquid ground state, avoids antiferromagnetic order and features a gap in the excitation spectrum (called the Haldane gap) which was discovered with neutron spectroscopy.[26] In contrast, S=1/2 antiferromagnetic Heisenberg chains have a gapless excitation spectrum consisting of fractional spin excitations,[27] but do not adopt long-range order even at zero temperature, but instead have a quasi-long-range ordered ground state. The slightest spin anisotropy orders a S=1/2 Heisenberg chain – a reflection of the fact that it is located exactly at a quantum critical point.

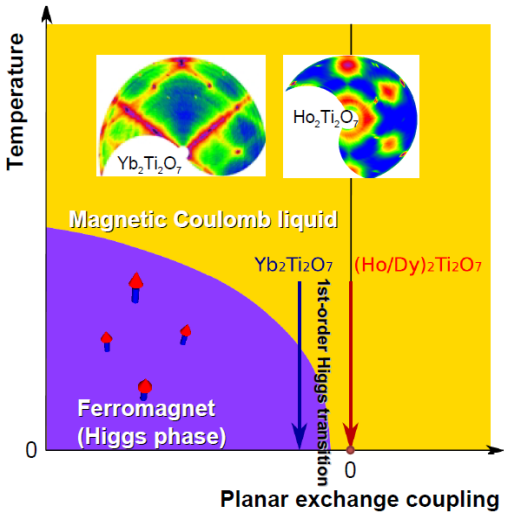

Figure 7: Higgs transition from an exotic magnetic Coulomb liquid to a ferromagnet in $Yb_2Ti_2O_7$.[32]

In the last 30 years, there has been tremendous progress in our understanding of magnetic quantum phases and quantum critical points in insulating materials. The notable examples include gapped systems, such as the Haldane chains or materials that are strongly frustrated, of which pyrochlore magnets are probably the best-known examples. In the simple case of weakly coupled quantum states that carry a magnetic moment, long-range magnetic order can be induced when the excitation is closed with the application of magnetic fields or hydrostatic pressure, as demonstrated for $TlCuCl_3$.[28] At the critical point, the material is completely governed by quantum fluctuations, features longitudinal fluctuations corresponding to the Higgs mechanism, and its ground states and its physical properties have no energy scale other than the temperature. It is interesting to study such phenomena in simple model systems because quantum critical points are believed to have a strong effect at non-zero temperature as well. In fact, in many materials, quantum criticality is thought to be

[26] W. Buyers et al, Phys. Rev. Lett. **56**, 371 (1986).
[27] D.A. Tennant et al, Phys. Rev. Lett. 70, 4003 (1993).
[28] C. Rüegg et al, Nature **423**, 62 (2003).

responsible for novel thermodynamic or transport properties.

Another important example concerns the pyrochlore magnets, where novel spin-ice ground states have been identified.[29] The ground state corresponds to a magnetic Coulomb phase featuring magnetic monopole quasi-particles that are stabilized by local constraints of a divergence-free flux. The EPS Europhysics Prize 2012 was awarded to a group of scientists who made heavy use of neutron scattering for their work. With the presence of enhanced quantum fluctuations, correlated quantum phenomena and novel magnetic order can emerge from the highly entropic magnetic Coulomb phase. In the spin-ice materials novel quasi-particles exhibiting the properties of magnetic monopoles determine the temperature-activated properties, and can be perceived as classical analogues of the spinons in one dimension. Quasi-long-range spin correlations are also observed in other pyrochlore magnets, giving rise to novel highly correlated states without conventional magnetic order that are only poorly understood. Case in point is $Tb_2Ti_2O_7$ that shows strong magneto-elastic effects and where novel low-energy magnetic modes have been discovered despite the absence of magnetic long-range magnetic order, part of which are of hybrid magneto-structural nature.[30,31]

One important focus in quantum magnetism is now on the three-dimensional frustrated magnets, such as the pyrochlores, where quantum effects can lead to highly correlated phases due to quantum fluctuations. Similar to the situation in one-dimensions, quantum fluctuations can be strong if the Hamiltonian contains so-called non-commuting terms that lead to strong fluctuations for simple arrangements of the magnetic moments. Quantum fluctuations are particularly strong if the magnetic moments are small, and/or if the magnetic interactions are dominated by exchange interactions as opposed to classical dipolar interactions. This leads to rich phase diagrams, separated by quantum critical points that can be accessed by tuning parameters, such as pressure and magnetic fields. For instance, in the quantum spin ice, magnetic monopole charges are carried by fractionalized bosonic quasi-particle spinons, which can undergo a Bose-Einstein condensation through a first-order transition via the Higgs mechanism.[32,33]

Other recent examples in the field of quantum magnetism include the observation of fractional excitations in spin ladder materials[34], and the discovery of E-8 symmetry in a ferromagnetic chain material $CoNb_2O_6$.[35] Polarized neutron diffraction, and quasi-elastic scattering, has played an important role in the identification of novel phases in condensed matter. The identification of three-dimensional spin-liquids in these and other materials will strongly benefit from magnetic diffraction studies of related phases using MAGiC, particularly from the polarization analysis over a large volume of reciprocal space.

With the increased scattering intensity expected for the proposed instrument, it will not only be possible to observe the order parameters, but also to determine the symmetry of the long-range magnetic order in such systems. In addition, many materials show incipient magnetic order in the form of short-range correlations, which have been beyond the scope of today's instrumentation. MAGiC will allow the simultaneous measurement of long-range ordered magnetic structures and short-range correlations, and provide a unique tool for the investigation of novel magnetic phases in materials. The availability of sub-Kelvin temperature sample environment, high magnetic field magnets and high-pressure cells will ensure its highest impact in the science community.

---

[29] T. Fennell et al, Science **326**, 415 (2009).
[30] S. Guitteny et al, Phys. Rev. Lett. **111**, 087201 (2013).
[31] T. Fennell et al, Phys. Rev. Lett. **112**, 017203 (2014).
[32] L.J. Chang et al, Nat. Comm. **3**, 992 (2012).
[33] K.A. Ross et al, Phys. Rev. X **1**, 021002 (2011).
[34] B. Thielemann et al, Phys. Rev. Lett. **79**, 020408 (2009).
[35] R. Coldea et al, Science **327**, 177 (2010).

Magnetism and ferroelectricity

Materials featuring both magnetic and ferroelectric order are important functional materials, which allow manipulating electric charges by applied magnetic fields and spins by applied voltages. Such materials have received enormous attention in the last 15 years as they open the road to new forms of multifunctional devices. Materials in which the ferroelectric and magnetic orders are associated with different ions represent an important class of **multiferroics**, so called *proper ferroelectrics*. As a consequence, materials potentially important for technological applications like $BiFeO_3$ (exhibiting the highest up to date electric polarization at room temperature) are characterized by a weak coupling of ferroelectricity and magnetism.[36] Stronger coupling can be achieved in *improper ferroelectrics* where the order parameter of the phase transition is not the polarization but another physical quantity. In these materials, spontaneous polarization arises in the phase transition as a secondary effect, for instance via electronic or magnetic correlations. Particular interest was attracted to magnetically induced ferroelectrics, which have been intensively studied since the discovery of ferroelectricity in $TbMnO_3$.[7] Ferroelectric polarization in this compound originates from a spiral magnetic ground state that breaks inversion symmetry[37], thus generating an electric field and ferroelectricity. Other mechanisms, like structural transition or charge ordering, that can yield magneto-electricity are now under intense investigation. Magnetic single crystal diffraction on MAGiC will be crucial for the identification of the underlying mechanism of multiferroic ground states.

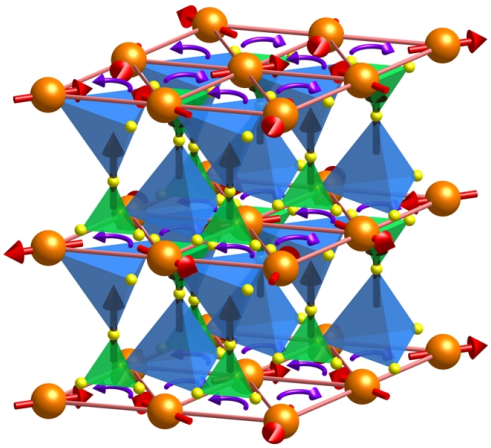

Figure 8: The multiferroic material $RbFe(MnO_4)_2$ featuring ordered magnetic moments (red arrows), truly chiral magnetic order (mangenta arrows) and ferroelectric polarization (blue arrows).

To date known improper ferroelectrics yield low polarization and transition temperatures, hence are unsuitable for technological application. New mechanisms are under consideration based on the use of hetero-structures in order to obtain high temperature multiferroics. Recently, a new route to ferroelectric ferromagnets was proposed by which magnetically ordered insulators, that are neither ferroelectric nor ferromagnetic, are transformed into ferroelectric ferromagnets using a single control parameter: strain[38]. The targeted system, $EuTiO_3$, was predicted to exhibit strong ferromagnetism and strong ferroelectricity. The proposed mechanism opens the door to higher-temperature implementations of strong ferromagnetic ferroelectrics, which would allow dramatic improvements in applications to materialize. Such materials showing strong spin-lattice couplings will be ideally studied with the proposed instrument. Other routes towards novel multiferroic mechanism may involve controlled disorder, which can introduce competing interactions and lead to uniform polarization.[39]

Magnetically-induced ferroelectricity offers great opportunities to study **magnetic chirality**. In multiferroic oxides, ferroelectric polarization arises from a noncollinear, in most cases chiral, magnetic order. The chiral magnetic states are the origin of their magnetoelectric and multiferroic behaviors.[40] In non-centrosymmetric crystals the magnetic chirality is governed by the structural one and can be

[36] G. Catalan, and J.F. Scott, Adv. Mat. **21**, 2463 (2009).
[37] M. Kenzelmann et al, Phys. Rev. Lett **95**, 087206 (2005).
[38] J.H. Lee et al, Nature **466**, 9331 (2010).
[39] B. Kundys, A. Maignan, and C. Simon, Appl. Phys. Lett. **94**, 072506 (2009).
[40] S-W. Cheong and M. Mostovoy, Nature Materials **6**, 13-20 (2007)

controlled by external forces. For instance it has been shown that the chiral component of the magnetic order can be poled by electric fields. Neutron scattering is a powerful tool to determine this absolute chirality but absolutely requires the use of **polarized** neutrons. The high neutron flux available at the ESS will allow considering compounds for which it is extremely hard to grow large size single crystals, or compounds with much lower amplitude magnetic density, broadly extending the range of materials to be studied such as molecular magnets or quantum magnets with very low spin values.

Magnetism in thin films and heterostructures

The epitaxial growth of single crystals offers great opportunity for materials science. Many modern materials applications require that materials can be made in a controlled and reproducible way. Epitaxial growth allows materials to be engineered with custom-made properties. What is also impressive are the novel properties that have been discovered at interfaces of thin films or domain walls where it appears that virtually every materials property can be achieved. Interfaces feature fundamentally new physics that can be induced by various reasons, such as vacancies, dislocations, strain, strain gradients or strong electric field effects. For example, two insulators give rise to a conducting interface layer,[41] that becomes even superconducting at very low temperature,[42] and electric fields can be used to tune the electronic properties through a quantum critical point.[43] The interface of an antiferromagnet may become ferromagnetic.[44] Domain walls in ferroelectrics can be conducting.[45] Strain can be used to engineer ferroelectric and magnetic properties.[46] Ferroelectricity can be induced by magnetic order in thin films.[44,47] Coupling such novel effects with the original bulk properties of the material can lead to novel functionalities.

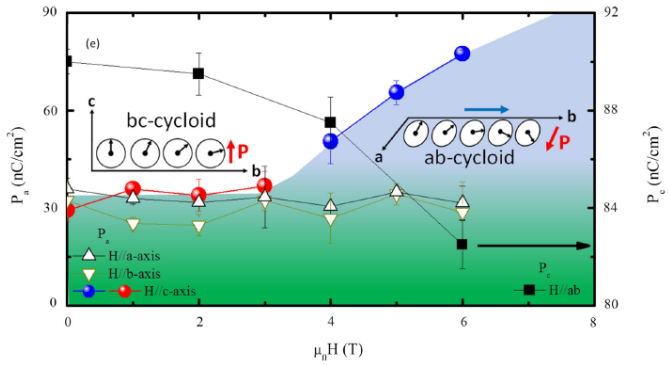

Figure 9: Ferroelectricity measurements on thin films of $TbMnO_3$. The magnetic cycloids in the pictures are the proposed magnetic structures as a function of magnetic field.[47]

Neutron diffraction has so far played a minor role in the study of thin film single crystals. Most of the neutron scattering work was performed using reflectometry, which is a powerful method to study in the depth dependence of the structure or the magnetization. There is at least 1000 times less material available for a neutron diffraction experiment on a thin film compared to a typical single-crystal experiment. However, recent results showed that simple studies are indeed possible even with today instrumentation.[48,44] With the improved performance of the proposed instrument, high-quality magnetic and structure determinations will become possible and make this technique attractive for a new community. One of the important advantages of the Laue time-of-flight method is that the thin films do not have to be first aligned, and a visual alignment will be sufficient. Given the relatively small intensities, that make the method much more accessible for the general user. Growing such materials in thin films offers the opportunity to strain-engineer some of the properties, and magnetic

[41] Ohtomo A, and Hwang HY, Nature **427**, 423 (2004).
[42] N. Reyren et al, Science **317**, 1196 (2007).
[43] A.D. Caviglia et al, Nature **456**, 624 (2008).
[44] J.S White et al, Phys. Rev. Lett. **111**, 3 (2013).
[45] J. Seidel et al, Phys. Rev. Lett. **105**, 197603 (2010).
[46] J.H. Haeni et al, Nature **430**, 758 (2001).
[47] I. Fina et al, Appl. Phys. Lett. 97, 232905 (2010).
[48] I. Gelard et al, Phys. Rev. B **92**, 232506 (2008).

neutron diffraction can play an extremely important role in this important field. In addition, it may also be possible to measure surface magnetic states in materials relevant for spintronics.

Antiferromagnetic (AF) thin films are now also widely used in spintronic devices (oxytronic), in which they play an important role by altering the coercivity of ferromagnetic layers through exchange bias. Yet in very recent reports, antiferromagnets are cast in a more active role. Indeed, both theoretical and experimental studies suggest that spin torque also exists within AF layers, with a much smaller critical current than in ferromagnetic layers. Furthermore, it has been recently shown that the switching of a magnetic order parameter could be achieved using a magnetic field pulse in a much more efficient way than for a ferromagnet. The rise of antiferromagnet spintronics thus poses an experimental challenge, since direct study of anti-ferromagnetic ordering is only possible through very few techniques. Of all techniques polarization analysis is the most direct one, giving access to magnetic ordering with no isotope limitations. With the high brilliance of the instrument, the ambition of MAGiC reaches out for parametric studies on epitaxially grown materials and even nano-patterned samples.

MAGiC will allow microscopic studies of antiferromagnetism in thin films and heterostructures. This will be complementary to neutron and X-ray reflectometry. It needs to be stressed that X-ray methods, particularly at energies of the relevant transition metal resonances, can usually access only a few magnetic Bragg peaks, and the penetration depth is limited. Magnetic neutron diffraction from thin films can probe the entirety of the thin film and will thus provide unique information about magnetic structures. It is also possible that MAGiC will be used to efficiently study lattice distortions in thin film crystals.

Novel long-length-scale magnetic structure

Magnetism can give also rise to new topological effects that may be useful for applications. Skyrmions are topologically stable spin textures that arise in the presence of spin-orbit interactions in a small set of chiral space groups. The name skyrmion is inherited from a hypothetical particle related originally to baryons.[49] They currently attract huge attention because they can be manipulated by electric fields with much lower current densities than multiferroics, opening the road to new electronics devices (based on topological Hall effect, spin transfer torque or spin Hall effect). Skyrmions are present in both metals and insulators alike : A Skyrmion lattice has been first observed in chiral metallic magnets, where the origin of the helical structure is due to Dzyaloshinsky-Moria interactions.[10] Small angle polarized neutron scattering played a prominent role in distinguishing skyrmion crystal from conventional triple-Q structure by observation of the second order satellites in the A-phase of MnSi (multiple number of Fourier components distinguishes the skyrmion lattice from a conventional triple-Q structure).[50] However, no quantitative comparison with theory was made, because of the difficulties for determining the absolute values of the scattering intensities in SANS. Similar studies performed around Bragg diffraction spots could lift the still existing ambiguity in distinguishing between skyrmion and multi-q models. However, the very high resolution and high flux needed in such experiments are currently unattainable. Such experiment can be envisaged on MAGiC in high-resolution mode.

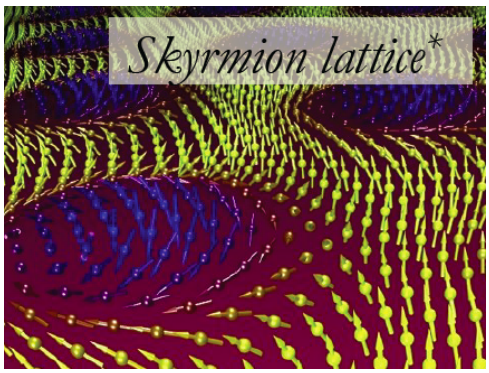

Figure 10: Artistic rendering of the magnetic structure of a skyrmion. The skyrmion twists extend over several nano-meters and are topologically protected, making them ideally suited for device applications.[10]

[49] T. H. R. Skyrme, Nuclear Physics **31**, 556 (1962)
[50] T. Adams, et al. Phys. Rev. Lett. **107**, 217206 (2011)

2. Instrument Concept and Performance

2.1. General concept

A rich variety of challenging science problems related to magnetic phenomena have been identified. Many of them require superior performance than current neutrons instrumentation provides, a performance that we target by the proposed instrument. Let us briefly summarize the key ideas, which guided the instrument design.

For single crystal diffraction at a pulsed neutron source the method of choice is **time-of-flight (TOF) Laue diffraction.** For most applications, and particularly when using the cold flux, the natural long-pulse of the ESS is very appropriate. However, for higher resolution requests, a pulse-shaping chopper can be applied. Since in general the long pulse width is very well suited for a TOF-Laue instrument, earlier reports already raised high expectations for this type of instrument at the ESS. If we assume TOF-Laue instruments at pulsed sources, which are ideally optimized with respect to their source parameters, the relative performance is determined by the ratio of their average brilliances; see Fig. 11, right. If one compares MAGiC with a Laue instrument say at ILL, we recognize a similar average brightness, at least for thermal neutrons. Transforming such instrument to a MAGiC-like TOF-Laue instrument will cost a factor 25, the ratio of pulse width to the ESS repetition time. This is equivalent with comparing their performance at the peak brightness (see Fig. 11, left).
As seen from the figures, comparing to the possibilities at other sources, gains of at least one order of magnitude are expected for a TOF-Laue instrument at the ESS, because of its high power and long-pulse structure.

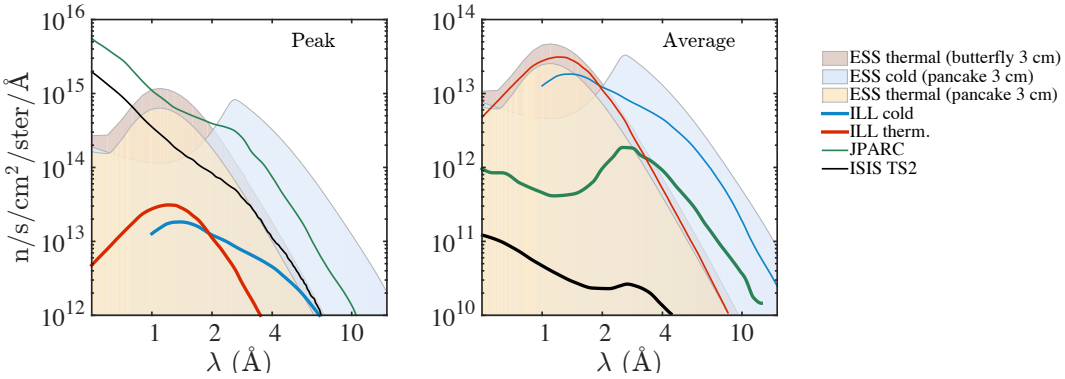

Figure 11: Peak and average brilliance of leading neutron sources compared to the ESS. (Data from a compilation of K. Andersen)

The science case shows distinct needs for thermal or cold neutrons and a MAGiC user will be able to choose between the optimized cold or thermal flux distribution. The lower wavelength limit of 0.6Å, which is reasonably achievable, will give a sufficiently large access to Q-space (Q_{max} <21 Å^{-1}, number of diffractions peak ~Q^3) for crystallographic and magnetic structure investigations, resulting in high structural resolution in real space. For many cases such as magnetic Bragg diffraction, parametric studies, diffuse magnetic scattering, the user can focus on a smaller Q-range (<6.2 Å^{-1}) with higher Q-space density and better Q-resolution, and by using the brightness of the ESS cold moderator.
In order to work at and push forward the frontiers in the science case of magnetism, polarization is a prerequisite. In a novel design and by means of modern neutron optics, MAGiC will provide in a very efficient way highly polarized neutrons over the whole wavelength spectrum. Without exception, the scientific case does not require for more than the natural bandwidth of ~1.7Å at 165m. The choice is best

suited to resolution and performance, and allows for high polarization of the used bandwidth. Within the divergence and phase space of interest defining the figure of merit, the neutron optics deliver approximately 80% of the (thermal and cold) source brightness.

The optimization is driven by requirements from challenging cases such as the scattering from weak magnetic moments and from very small single crystal samples. There is a major challenge with the high gain of the TOF-Laue instrument that is mandatory to address: without improving the signal to background ratio these gains could be pointless for the most challenging cases. A clean focusing for smallest samples and avoidance of undesirable scattering are examples, which of course received special attention. The need for revealing very weak elastic scattering, or for studying the intrinsic quasielastic nature of spin-liquid diffuse scattering, can be met by using optionally a monochromating chopper with one to few percent duty cycle.
However, the ideal and most important tool to reveal weak magnetic diffraction signals of interest can be found by using polarized neutrons. Polarization is a special gift in magnetic scattering, as it enables the separation of magnetic scattering from nuclear scattering and background, and the higher the polarization the better the separation. Polarization is not only important to suppress background close to extinction, but also to reveal a weak magnetic signal on top of a nuclear Bragg peak. Polarization supports the central part of the science case that is related to the directional vector properties of magnetic moments, and reveals magnetic scattering terms and properties, which otherwise remain hidden in unpolarized experiments. Therefore, we propose a dedicated polarized instrument.

MAGiC is a novel instrument solution using neutron optics to provide nearly ideal polarization with high efficiency for thermal and cold neutrons.

2.2. Components

An overview of the instrument scheme is depicted in Fig. 12. The neutron optics use a vertical focusing element in the monolith, a solid-state bender outside the monolith near to the pulse shaping chopper, and a double elliptic guide kinked out of direct line of sight. The solid state bender and one of the vertical sides of the neutron guide can have FeSi supermirror coating for beam polarization. The chopper system defines the wavelength frame and time resolution with large flexibility. There are two position sensitive detectors, a larger one (2.8 sr solid angle) and a smaller one (0.2 sr) equipped with supermirror polarization analyzers.

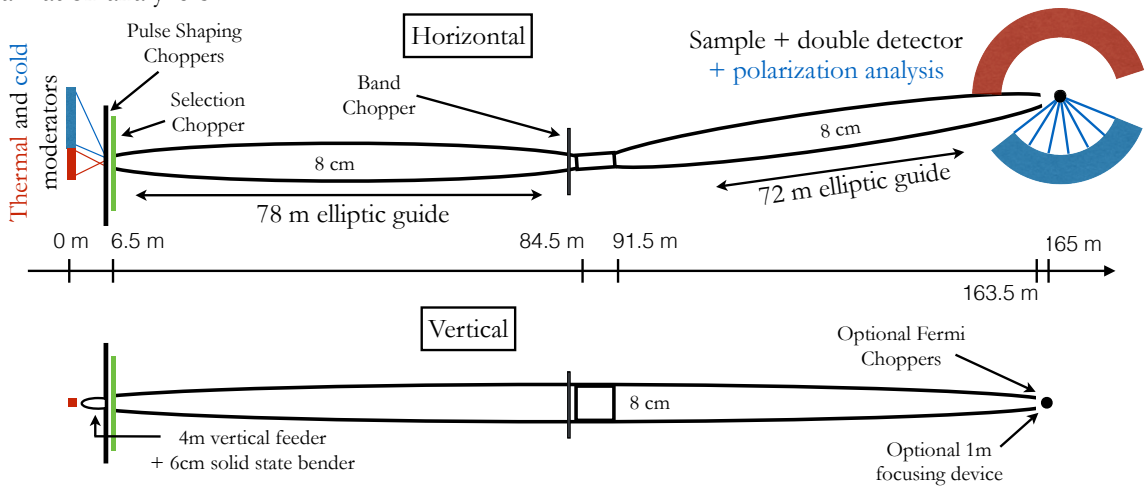

Figure 12: Schematic layout of the instrument showing the guide system and the chopper positions in a horizontal and vertical cut (*top* and *bottom*, respectively). PSC and BC denotes Pulse Shaping Chopper and Bandwidth Chopper. A solid state bender near to the PSC, can be moved in to reflect cold neutrons into the guide.

2.2.1. Neutron optics, transport and polarization

Moderators

All optimizations concerning neutron transport have been made using the so-called **pancake moderator** as designed in 2014. The reduced height of this moderator yields an increase of brightness compared to the Technical Design Report for both thermal and cold spectra. This moderator has a height of only 3 cm, a cold moderator diameter of 24 cm next to the thermal wings, each of 12 cm width. The beam ports offer a view to both thermal and cold moderators being placed next to each other. We therefore optimized our instrument by investigating geometries allowing for alternate use of thermal or cold spectra. The first part of the double-elliptic guide will directly view the thermal moderator, and for switching the view to the cold moderator, a solid state bender made of Si-wafers will be moved into the beam. With a polarizing FeSi coating the cold neutron beam is injected into the main guide system with high polarization.

We may note that very recently, the baseline for moderators has been modified again. The MAGiC instrument will in particular benefit by a gain of about 100% in the thermal spectrum compared to the pancake moderator, which was chosen in our simulations, see Fig. 11. There is practically, no further change for the cold spectrum. Note that this gain is not yet included in the given flux numbers.

Neutron optics and guide system

The neutron optics has been optimized for a figure of merit (FOM) given by a maximal sample size of 10 mm height and 10 mm diameter, and a incident divergence of +/-0.3° in both directions.

The neutron guide system, schematically shown in Fig. 12, consists of a 4m long "feeder" guide element in the monolith, that is vertically focusing on the 3cm high pancake moderator, followed by two elliptic sections, of 78m and 72m length, respectively. The elliptic sections have a maximal cross section of 8cm×8cm and are connected by a straight 6m long section. The elliptic sections are kinked by 0.2° at both ends of this part for the purpose of avoiding direct line of sight and ensuring high polarization with excellent brilliance transfer (see below). Outside the monolith, there is a ~50 cm gap to place the solid-state bender and the pulse shaping chopper system. The total instrument length is of 165m.

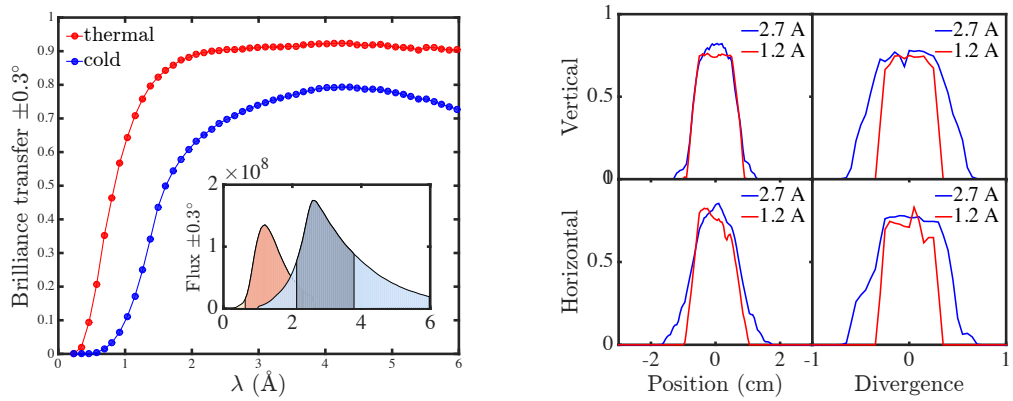

Figure 13: *Left:* brilliance transfer for the thermal and cold moderator in the divergence ranges of interest. Inset: unpolarized flux at sample position. Grayed areas correspond to the effective bandwidth of use. *Right*: beam shape (left) and divergence (right) for both moderators maximum wavelength at sample position.

Optimizations have been made using McStas 2.1 with gravity taken into account. The optimized guide solution presented above has been tested with super-mirrors with up to m=4 coating. The resulting

brilliance transfer curves, focal properties and divergence profiles are reported in Fig. 13 and show excellent performance. The corresponding flux curves are shown in the insert of Fig. 13. Here the shaded areas indicate our choices for the wavelength band, choosing either the maximum of the thermal or the cold moderator flux distribution, and using either 85% or 60% of the total available thermal and cold neutron spectrum, respectively. Obtained divergence and beam size match the requirements of homogeneity on the 1cm^2 surface at the sample position. Additional optimizations of *m*-coating distribution along the guides have been carried out using McStas,, to minimize the total guide cost and to reduce background at sample position. The effective *m*-coating will be between 1.5 and 5, the highest being located at the beginning and end of both ellipses as well as on the reflecting side of the straight element.

Solid State Bender

Injection of cold neutrons into the guide is made via a 6.05 cm solid state Si-bender matching the guide opening (2.5x4 cm^2) and placed at 6 m from the cold moderator. The bender is made of 167 vertical 150 μm channels with the curvature radius of 3 m in order to escape the direct line of sight. It has a take-off angle of 1.3° adapted to the moderator geometry. McStas simulations show a transmission of ~90% between 2 and 4 Å, which slightly decreases above 4 Å (~80% at 6 Å) due to the wavelength dependence of silicon absorption.

Neutron Polarization

Polarizing supermirrors, either in reflection or transmission, and ^{3}He filter cells are the standard means for polarizing a polychromatic beam. Accepted divergence and absorption of both devices depend on wavelength and it is usually unfeasible to cover the whole required wavelength spectrum with a single device.

Polarizing cold neutrons: For cold neutrons the performance of supermirrors is usually superior. The best performance with very high polarization and transmission is found for a polarizing bender that is made of a Si-wafer stack coated with a FeSi supermirror [51]. For MAGiC the best polarization and brilliance transfer is achieved, if this device is placed in the focal point of the first elliptic guide element. A compact FeSi bender device of 6 cm length can be placed outside the monolith to inject polarized neutrons from the cold moderator. The expected polarization is above 99% over the whole wavelength range, while the mean brilliance transfer is close to 42%. The full unpolarized cold neutron flux can be obtained by an additional bender using a non-polarizing NiTi coating and same geometry combined with a non-polarizing guide (NiTi) guide.

The device can be removed out of the beam, when operating with thermal neutrons and easily replaced in case of failure. Guide fields along the beam path preserve the high polarization. A further advantage of this setup is that the beam homogeneity, focus and divergence at the sample are independent of the bender and only determined by the very good optical properties of the focusing elliptic guide.

Polarizing thermal neutrons is more challenging. For MAGiC two options were considered:

(i) Unpolarized guide in combination with removable ^{3}He filter cell
(ii) Polarizing guide with FeSi supermirror coating of vertical walls

Both options are feasible and are of interest. The final choice will also depend on ESS resources for operating He-3 polarizers and will not be decided before phase 1.

[51] Th. Krist, F. Rucker, G. Brandl, R. Georgii, *NIMA* 698 (2013) 94.

Option (i) is based on a conventional non-polarizing NiTi coated double elliptic guide associated to a SEOP cell with pressure and length optimized for short wavelength of 1.2 Å. Typical figure of merit P^2T of such a device is shown in Fig. 14. The cell gives 86% polarization (P) at 30% transmission (T) and has to be removed when using unpolarized neutrons. The cell is sensitive to magnetic stray fields and needs to be shielded. The SEOP cell can be provided for construction of MAGiC by JCNS.

Option (ii) is a polarizing guide system using FeSi coating (which avoids the strong Co-activation of FeCoV). The polarizing FeSi guide removes the possibility to use the full unpolarized source flux on the instrument. However, the achieved flux in polarized mode is 2.5 times higher than for option (i). Performances of the two options are shown in Fig. 14.

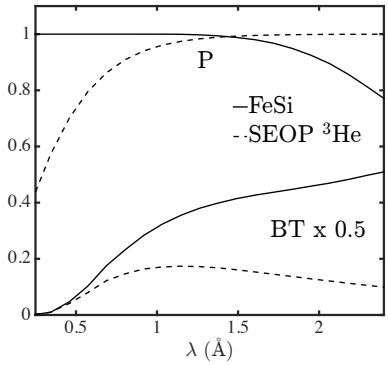

Figure 14: Comparison for polarizing thermal neutrons by guide optics (lines) and SEOP ^{3}He filter cells optimized for 1.2Å (dashed lines, data given by courtesy of Earl Babcock).

Flux numbers

The performances of the neutron optics and polarization in terms of flux on a 1cm² sample are summarized for the two options below:

λ (Å) (divergence)	Flux(n/s/cm²/1.7Å) option 1	polarization option 1	Flux(n/s/cm²/1.7Å) option 2	polarization option 2
0.6 – 2.3 (±0.3°)	0. 45 × 10^9 2.2 × 10^9	0.97	1.1 × 10^9	0.96
2.0 – 3.7 (±0.5°)	4.3 × 10^9 8.6 × 10^9	0.99	4.3 × 10^9	0.99
3.7 – 5.4 (±0.5°)	2.2 × 10^9 4.4 × 10^9	0.99	2.2 × 10^9	0.99

Blue numbers correspond to the unpolarized flux expected using option (i). The option (i) using a non-polarizing guide gives twice higher unpolarized thermal and cold flux. The polarized thermal flux is ~35% of what is obtained with option (ii). The average polarization in both cases is similar, however, supermirrors show better performance at shorter wavelengths. Removing the ^{3}He cell out of the beam provides the same polarized cold flux as with option (ii)

Focusing and slit system for small samples

An important ability of MAGiC is to study sub-millimetric samples. Therefore, we use an extension of the guide system[52] by a 1m elliptic focusing element (coating up to m=7). Simulations show that the guide system including the focusing option is able to deliver a homogeneous divergence profile with an efficient high brilliance transfer for a divergence up to +-0.8° (fig. 15) on a 1 mm² area. The integrated flux increases from 1.1x10^9 n/s/cm² to 5.8 x10^9 n/s/cm² in the thermal range corresponding to a 5.2 gain factor. To limit divergence and spot size at the sample position, a double pinhole system[53] is finally placed within the last 0.5 m between the focusing device and sample position[54]. For high-field magnets, the collimation device needs to be integrated into the magnet and close to the sample. The motion control for alignment can be based on (attocube) piezo-electric motors, which operate at low temperature and under high magnetic field.

[52] There are possible further improvements for focusing by adapting the total guide system in the optimization.
[53] See Espresso proposal
[54] "*VacBox*", A. Hiess *et al.* ICNS 2013

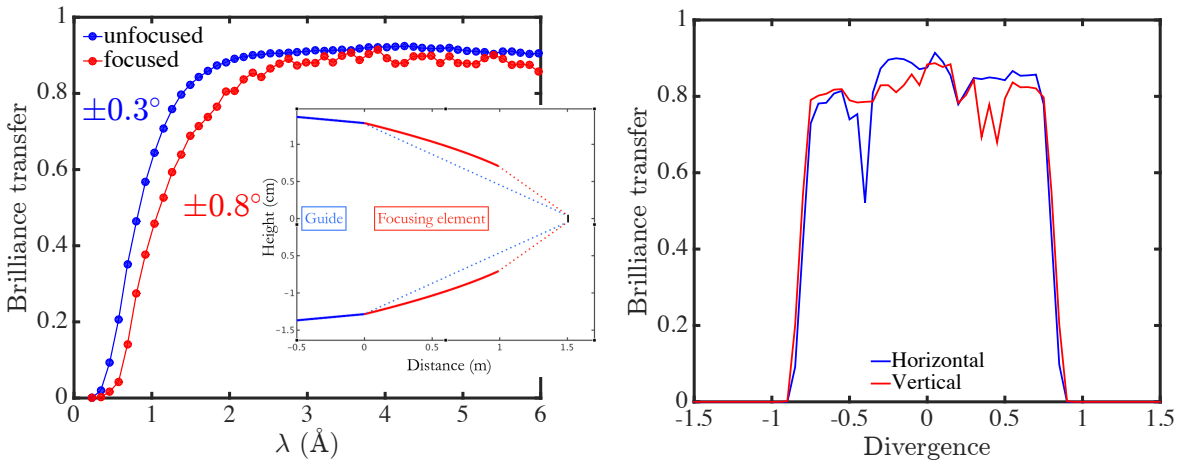

Figure. 15: *Left:* Brilliance transfer curves of the non-focused (blue) and focused (red) version of MAGiC over a 1 mm² surface. Focused brilliance transfer is close to the optimum. *Inset*: sketch of the elliptic focusing element. Dashed lines show the increase in divergence induced by the focusing. *Right*: divergence profiles for a 1 mm² square surface.

2.2.2. Chopper system

The chopper system consists of (i) two counter-rotating pulse shaping disc choppers (**PSC**) at 6.22 and 6.24 m, (ii) one 14Hz pulse selection disc chopper (**SC**) at 6.7 m to assure to have no leakage and cross-talk of undesired wavelengths, (iii) one 14Hz band control disc chopper (**BC**) at 75 m, which defines more precisely the wavelength band for the TOF frame at the detector position. and (iv) an optional Fermi chopper (**FC**) 75cm before the sample, monochromating the beam for a multiple set of wavelengths.

(i) The **PSC** uses a disc diameter of d=45cm (to stay within the 5°sector) and operates usually below 200Hz. The beam cross-section at the PSC is 2.5cm in width and 5cm in height. The chopper opening is chosen to 5cm width. For a slit width of 5cm and counter-rotation with 168Hz and 182Hz this yields 0.15ms pulse width, as needed for the best resolution. With an additional 120° opening segment on both counter-rotating discs, it is further possible to achieve a rather favorable wavelength-dependent pulse shaping as shown in the acceptance diagram versus t and λ (fig. 16). Rotating at 112Hz, the beam is opening within 0.1ms. The action of the PSC in the latter case can be seen as only opening, while closing is determined essentially by the end of the ESS pulse.

(ii) The **SC** operating at 14 Hz is placed next to the PSC to assure an effective opening only with the 14 Hz source frequency. Its diameter is (30cm to) 45 cm and its rotation axis is above the beam, a configuration, which yields short opening/closing time of (2ms to) 1.3ms.

(iii) The **BC** operating at 14 Hz is placed at 75 m with a 180° window on a disc of 70 cm diameter.

(iv) The two **FC**s are an option and can be moved in at 75cm near to the sample and closely next to each other in a common housing. The slit package consists of a Si-wafer stack covering a beam cross-section of 23×23mm². The two FC provide different resolution setting with large flexibility; in combination of both FC the repetition rate and resolution can be decoupled. The thickness of each wafer is d=280μm and 420μm for the first and second FC respectively. Both FC have a length of l=6.6mm and operate at frequencies up to 672Hz (=48×14Hz). The combination provides flexibility with repetition rates from 24 to 96 frames of 0.74ms to 3ms and pulses of 20 to 60μs. The FC slit package is made of Si-wafers, which are sputtered with 3μm layer of ^{10}B on top of a 2μm layer of Gd (a combination for lowering the high-energy γ production and $<10^{-6}$ background suppression).

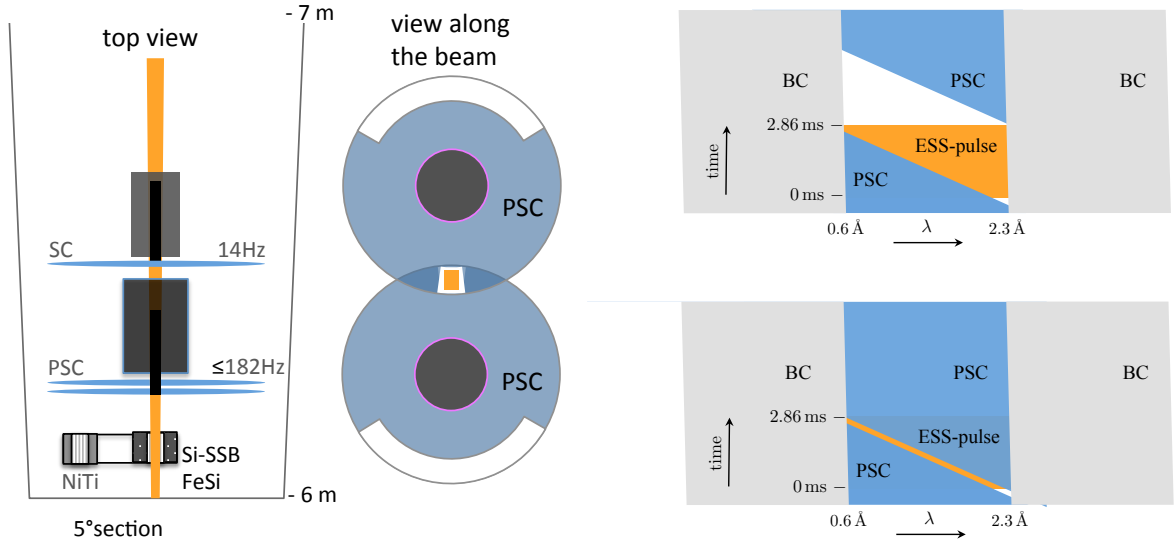

Figure 16: *Left*: Top and front view of the chopper system near the monolith, pulse shaping choppers consisting of counter rotating pulse shaping choppers (PSCs) and the 14Hz selection chopper (SC).. The beam is shown in orange. *Right*: Acceptance diagram time versus λ, illustrating the wavelength dependent pulse shaping for thermal neutrons, (top) asymmetric pulse profile to improve the time resolution particularly for high Q diffraction using the large PSC opening, (bottom) constant 0.2 ms high time resolution using the small opening as shown in view along the beam.

2.2.3. Secondary instrument

The scheme of the secondary instrument is depicted in Fig. 17.

There are two typical modes, one with a high field vertical magnet at sample position for field dependent studies and a second with xyz-fields for defining and tuning the direction of the initial polarization. The instrument will be made of a large detector particularly for Laue applications, and of a smaller one for polarization analysis. The large detector can also be used for half-polarized experiments and a further second detector for probing simultaneously a subset of data with polarization analysis. The scattered flight path between sample and detector is in-housed with an Ar or He atmosphere for background reduction. Both detectors can be rotated to give access to small Q either with or without polarization analysis.

Detectors

There will be two 1m radius cylindrical detectors, left and right to the beam axis. One of these will be a large detector with 160° horizontal and +/- 30° vertical acceptance, covering a solid angle of 2.8sr. The large solid angle is particularly important for the Laue-TOF method and is adapted to the opening of the vertical 8T magnet. The second detector will have a 120° horizontal and a smaller +/-3° vertical acceptance with 0.2 sr solid angle coverage, which adapts to the geometry of the supermirror polarization analyzer. The requested spatial resolution is 4x4mm² for both detectors.

The best detector choice for the single crystal diffractometer MAGiC is similar to the DREAM proposal: This is a ^{10}B based volume detector with inclined geometry of the Jalousie detector concept[55]. A prototype has been built and successfully tested for POWTEX at MLZ. The detector has a 3D grid of detection cells, working in coincidence mode of anode and cathode signals, rather insensitive to γ-background. The

[55] G. Modzel et al. *NIM* A **743**, 90–95 (2014).

cathode layers are coated with 1µm ^{10}B and are set in inclined geometry (10°), which with several layers are shown to yield measured detection efficiency larger than 50% at 1Å [1]. There are favorable features of this volume detector: the distribution of counts into ~20 cm detector depth yields higher count rate capabilities, while the resolution can be appropriately chosen to ~4 mm (FWHM), the surface projection of the 3D cells provides an effective finer pixel mesh (~1x1 mm^2) and finally, the concept offers new possibilities to discriminate background from sample environment by the intrinsic collimation.

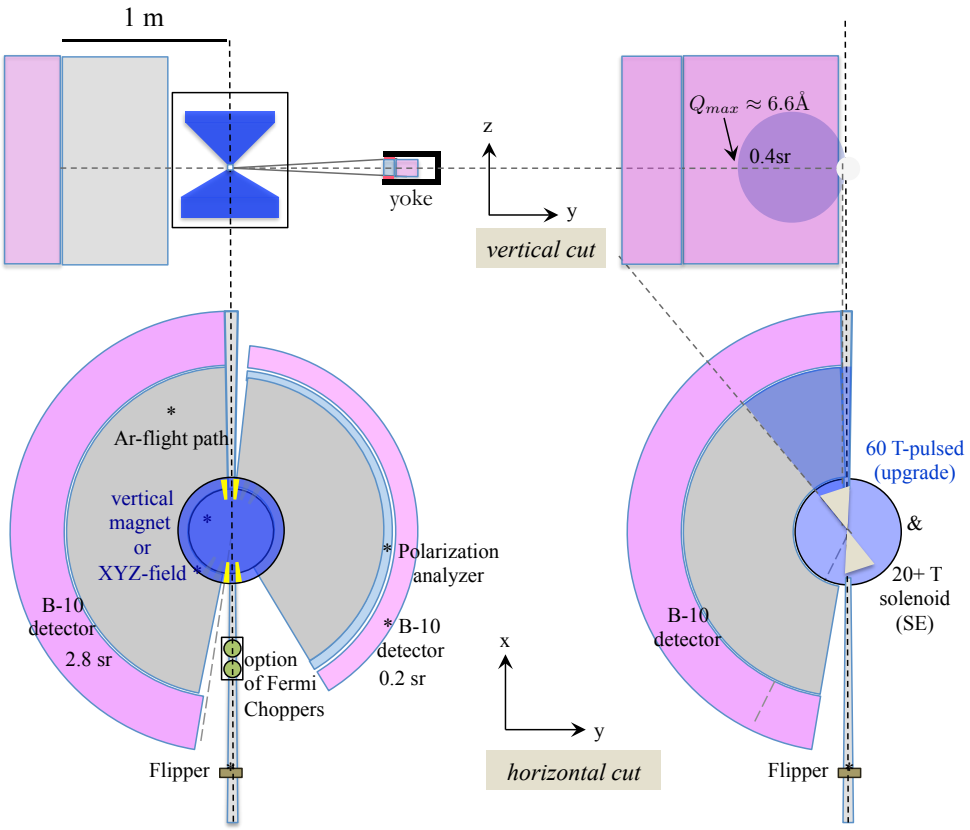

Figure 17: Scheme of the secondary instrument and its components (1 m scale see top left).
(left) vertical and (right) horizontal magnet and detector acceptance.; (top) vertical cut (bottom) horizontal cut.

Devices for Polarization Analysis

The scheme for longitudinal (xyz) polarization analysis requires an (i) initial polarizer, (ii) π-flipper, (iii) xyz-field at the sample, (iv) guide field, and (v) polarization analyzer.

(i) Here, the initial polarizer is realized for thermal neutrons either by the polarizing guide or a SEOP He-3 filter cell and for cold neutrons by a polarizing bender[56] near to the PSC, see above.

(ii) There are various possible choices of a π-flipper. One is a so-called Mezei-type rectangular coil set, as used at DNS or D7. For using a broad band of wavelength, the Larmor-precession field of the flipper will be ramped with time following the wavelength-time dependence of the incoming neutrons, as done on the Jülich spin-echo instrument at the SNS. The alternative for a π-flipper is an adiabatic fast passage (AFP) RF flipper. A He-3 polarizer could include the AFP flipping, see [57], for a cryoflipper, see[58].

[56] C.F. Majkrzak *Physica B* **213&214**, 904 (1995)
[57] S. R. Parnell et al., *NIMA* **722**, 20-23 (2013), Physics Procedia **42**, 125-129 (2013)

(iii) The xyz-field coils will be used in absence of a magnet around the sample with sufficient space to place a standard orange-type cryostat (see design for xyz-field of TOPAS at MLZ).
(iv) In order to preserve the polarization, there will be a permanent guide field along the vertical z direction compatible with the field of the magnet at the sample position.
(v) For polarization analysis, there are various options available that are based on supermirror polarizer, which have the advantage of an easy operation, of compatibility with a (compensated) magnet at the sample, and of high polarization. Currently, there are wide-angle polarizers at three instruments D7 (ILL), DNS (MLZ) and HYSPEC (SNS), and they are all made of Boron-float glass (0.2mm) coated with supermirrors (m~3) and air gaps (~1mm) for neutron passage. Among these, the most recent HYSPEC-polarizer (built at PSI) uses only a single frame without blind regions over the whole analyzer area (see Figure 18). One may note the particular expertise in the proposal team on polarization analysis. There is interest by PSI and JCNS to explore new developments including the prototyping for a wide-angle polarizer, using Si-wafers with FeSi supermirror coating. Here, the same concept [50] as for the initial polarizer should provide a homogeneous response suitable for quantitative determination of Bragg intensities and a larger Q-range with a minimal wavelength of 2 Å by a supermirror coating of m=3.2 Blind regions in the analyzer for frames or field assembly are an issue especially for monochromatic instruments and should be minimized even though this is less important for MAGiC using a continuous wavelength band. The return fields will be closed either to side of the polarizing supermirror (see Fig. 18) or enclose the detector (similar to D7). Preliminary studies indicate that modifying the sputtering process can significantly reduce the required field strength. We consider different assemblies of the Si-wafers, in S-bender, bender or mirror-stack geometry. A wedge-type shape of the short wafer pieces is possible but actually is not needed, since the slightly convex shape for the polarizer stack can be achieved with 5 μm Al-foil spacers. The construction of the polarization analyzer is a possible in-kind contribution by PSI.

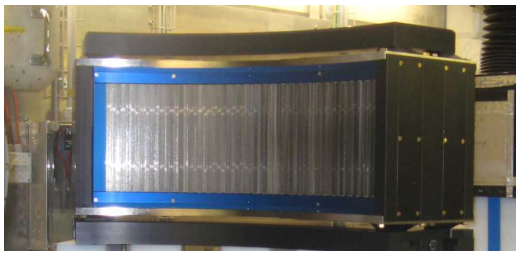

Figure 18: wide-angle supermirror analyzer at HYSPEC

The instrument can offer further *spherical polarization analysis* and access to the off-diagonal elements of the polarization tensor of incoming and final polarization. Therefore, one needs to operate the flipper coils in $\pi/2$ mode, which initiates a precessing incoming polarization in phase with the incoming wavelengths like for the SNS spin-echo instrument. The precession phase given by the field integral along the path from the flipper to the sample can be compensated by a reversed field – like by a spin-echo coil – and further set to any direction perpendicular to the field orientation of the xyz-coil. Measuring the final polarization parallel to the field at the sample now will determine off-diagonal terms[59]. The use of the spin-echo coil is a simple new idea with respect to an earlier experimental set-up on the DNS[60]. It should ease the use of the proposed method significantly as it should improve its accuracy[61].
The separation of scattering terms from single crystals by polarization analysis is straightforward and fully established.[62] It is an extension of the original xyz-method of Schärpf for powder averages.[63,64]
In combination with energy analysis, the polarization analysis with supermirrors can be used for final energies < 20 meV and will cover well the needs for quasi-elastic diffuse magnetic scattering and true elastic scattering for Q<6Å.

---

[58] Th. Krist, F. Rucker, G. Brandl, R. Georgii, *NIMA* **94**, 698 (2013)
[59] E. Babcock et al., *Physica* B **397**, 172-175 (2007)
[60] W. Schweika, *Physica* B **335**, 157 (2003); W. Schweika, S. Easton and K.U. Neumann, *Neutron News* **16**, 14 (2005)
[61] W. Schweika, ICANS 2012
[62] W. Schweika, *J. Phys.: Conf. Ser.* **211**, 012026 (2010)
[63] O. Schärpf and H. Capellmann, *Phys. Status Solidi* a **135**, 359 (1993)
[64] G. Ehlers, J.R. Stewart, A.R. Wildes, P.P. Deen, K.H. Andersen, *Rev. Scient. Instr.* **84**, 093901 (2013).

The alternative ^{3}He polarization analysis is of preferred interest for polarization analysis of thermal neutrons, i.e. for diffraction at Q>6.2 Å^{-1}. A ^{3}He banana-type filter cell around the sample may provide polarization analysis also for the larger detector within a vertical range of +/-20° (see TREX proposal). Interesting applications can also be seen for another community in the separation of coherent and incoherent scattering of hydrogen in soft matter. We consider a ^{3}He analyzer as an *upgrade option*.

Sample environment

Magnets:
Superconducting split-coil magnets with fields up to about 15 T are commercially available and in operation at many neutron and synchrotron facilities. An 8T split-coil magnet (NbSn based) with wide angular aperture (such as 60° vertical, 300° horizontal) is planned to be available from the sample environment (SE) pool. It will make full use of the 2D detector and is compatible with polarization analysis at ~1m distance. The cryogenic insert of the magnet will be equipped with a non-magnetic goniometer for easy sample orientation. There are also plans by SE to provide a high field horizontal magnet with symmetric openings of +/-20° on both sides. The magnet configurations are depicted in Fig. 17, including the foreseen upgrade of the pulsed magnet.
There will be an instrument-dedicated magnet, which is planned to be ready for operation after the commissioning phase of MAGiC 2023. The asymmetric split-pair design should yield as high as possible vertical field for rather small samples, which allows for relaxing the demands for field homogeneity, and for possibly less vertical angular aperture. We shall also consider the possibility to develop and share use and costs for this very-high field magnet with CAMEA.

Magnets:	Opening angles	Field	Resource	Time
Vertical split-coil	~160° × ~60°	~ 8 T	SE	2023
Vertical split-coil	~160° × *tbd*	$\lesssim$ 20 T	MAGiC/CAMEA	2023
Horizontal solenoid	$\pm 20°_{in} \times \pm 20°_{out}$	$\gtrsim$ 20 T	SE	2023
Horizontal solenoid	$\pm 15°_{in} \times \pm 30°_{out}$	~60 T pulsed	MAGiC	Upgrade

Cryogenics:
The sample station will be designed to accept cryogenic equipment from the sample environment group. All generic liquid ^{4}He cryostats, dilution fridges and furnaces will be used on occasion. Temperatures in the 50 mK - 1000K range will be available to users. Our dedicated superconducting magnet will use various inserts to match the experimental requirements. A dedicated dilution fridge will be specifically designed. These inserts will be part of the beam line cost. Temperatures in the range 30 mK - 300K will be available under magnetic field to the users. Experiments under pulsed magnetic fields using a dedicated LN_2/He cryostat are an upgrade option.

High Pressure:
MAGiC will be fully compatible with the use of various pressure cells. We do not plan to develop a specific pressure setup; however we will make full use of the "sample environment group" expertise on this matter to fulfill user needs.

2.3. Performance and benchmarking

MAGiC is supported by a huge and diverse science case for which multiple operation modes are mandatory. Its design has been made with flexibility in mind, allowing for shifting the wavelength band, fine-tuning flux, resolution and Q-range, and for adapting to very small sample size. In the following, we will present MAGiC capabilities for various science case simulations.

2.3.1. Simulations of experiments

In this section, we shall illustrate the MAGiC performances simulating experimental results with various sample sizes, polarization, resolution and Q-range.

Standard nuclear and magnetic structure determination

To illustrate the MAGiC ability to refine magnetic structures, we have simulated the whole instrument and performed a virtual experiment on a hexagonal multiferroic compound $HoMnO_3$ (a=6.14 Å and c=11.41 Å). $HoMnO_3$ orders in a non-collinear magnetic structure with a $\mathbf{k}$=0 propagation vector and a magnetic moment of 3 μ_B on both Mn and Ho sites[65]. In our simulation we considered spheres from 0.001 to 10 mm^3 volume. Laue patterns were simulated using the larger detector bank by rotating sample around the c-axis with 2° steps, using full pulse width and an exposition time of one second per pattern for samples larger/equal than $1mm^3$. Simulated 180 Laue patterns were converted in the three-dimensional (3D) reciprocal space of the crystal. The resulting integrated intensities are the sum of both P+ and P- corresponding to an unpolarized measurement. Finally, no instrumental background has been simulated; however we increased the acquisition time by a factor 3 in order to fairly account for electronic, hot neutron, sample environment background and detector efficiency. The background issue will be discussed further on in the following parts of the proposal.

The results of the simulation are reported in Fig. 19 showing a 2D cut of the data in the (hk0) reciprocal lattice plane. We used thermal neutrons from 0.6 to 2.3Å and a $10mm^3$ sphere of $HoMnO_3$. As can be seen, pulse shaping is not required for this case to integrate the sufficiently resolved peak intensities. Switching to the cold moderator yields ten times fewer reflections due to the smaller Q-coverage, however, with 5 times higher integrated intensities.

Various sample sizes and ordered magnetic moment were simulated in order to reach the limits of MAGiC. The complete results list is reported in Table 1. Down to a cubic millimeter crystal size and 1 μ_B moment, an acquisition time of a few minutes will be sufficient to refine both magnetic and nuclear structures.

Table 1: Number of useful Bragg reflections (>3σ) collected on MAGiC for various *b*-HoMnO3 sample volumes.

	10 mm^3/3 μ_B / 9 min		1 mm^3/3 μ_B / 9 min		10^{-3} mm^3/3 μ_B / 180 min	
	Nuclear	Magnetic	Nuclear	Magnetic	Nuclear	Magnetic
Cold moderator	372	274	274	236	177	108
Thermal moderator	4713	818	1534	341	346	43

For micrometric samples, the full diffraction pattern acquisition will be obtained in a few hours confirming the high potential of the single crystal Laue-TOF method. These performances will open the road to the study of micrometric (synchrotron) samples or strongly diluted magnets. On top of the structure refinement, experiments under magnetic field could also benefit of the strong beam polarization for free, allowing spin density and local anisotropy refinement.

[65] X. Fabrèges *et al.*, *Phys. Rev. Lett.* **103**, 067204 (2009)

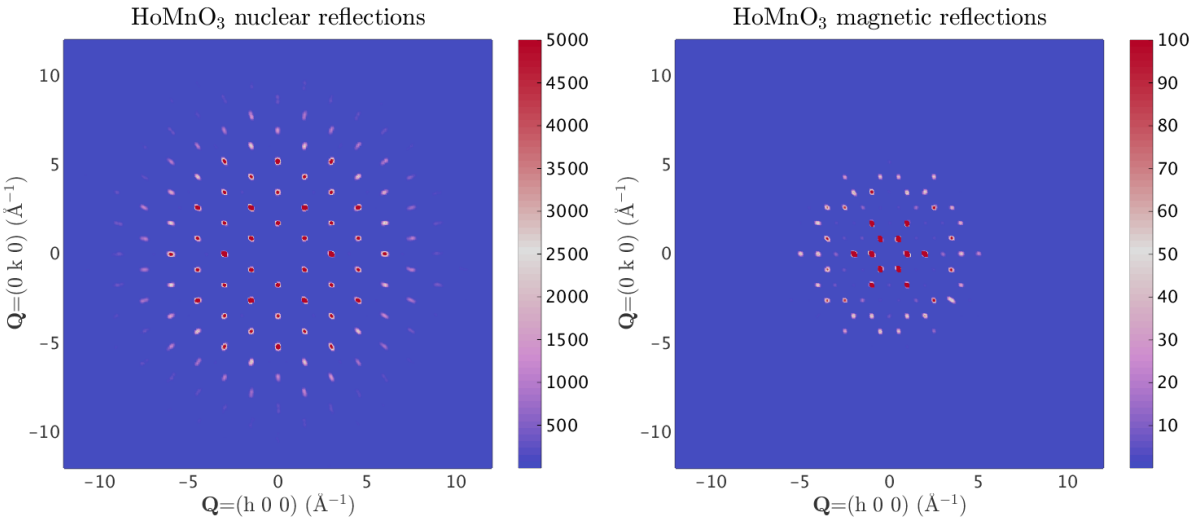

Figure 19: $HoMnO_3$ two dimensional cuts of the reciprocal space (hk0) as obtained on MAGiC in 180s exposure time. Bragg peaks are well resolved both on nuclear (left) and magnetic patterns (right) and can be easily integrated.

The TOPAZ experience in current TOF-Laue experiments

To validate our simulations, we performed an experiment on TOPAZ at SNS. TOPAZ is a Laue-TOF single crystal diffractometer dedicated to crystal structure studies. It has large detection coverage on one of the most advanced spallation source in operation. In this respect, it is of interest to show the possibilities of this instrument type and to compare the performance of TOPAZ with MAGiC. One should note however, that TOPAZ is not particularly dedicated for science cases related to magnetism. It cannot cover the needs for low temperatures or high magnetic fields (Anger camera detectors) and does not offer polarized neutrons.

The experiment was made on a chain/ladders compound $(La_xSr_{14-x})Cu_{24}O_{41}$. We made a simulation of the same experiment on MAGiC using the nuclear structure factor obtained on TOPAZ as an input to confirm the validity of our estimated counting time. Based on SNS flux and repetition rate, we estimate a gain factor of 60 for MAGiC on counting rates. Our simulation showed that an 11 min acquisition was sufficient to obtain the 12 hours counting statistics of TOPAZ. It corresponds to a gain factor of 66, close to the expectation. This result alone confirms the quality of our simulations. Note, the gain factor relates to the specific although typical case for magnetic structure determination. On the other hand, MAGiC is not designed for high-resolution crystallography experiments, where the short pulses and short wavelength neutrons available at SNS make TOPAZ highly performing.

More details on the comparison with TOPAZ are given in the Appendix A.

Structure determination on very small single crystalline samples

There are numerous examples, where crystals of large size simply cannot be grown due to complex synthesis. Another case is set by the need for high pressure. Reaching dozens of GPa limits the sample volume to the diamond anvil one. In both cases, additional focusing could be desirable. In our simulations, we typically used a 10^{-3} mm^3 volume as a reference. To partly compensate for the low sample volume in the beam, one made use of the additional focusing device, relaxing the divergence to 0.8^ox0.8^o on a 1 mm^2 beam cross-section at the sample position. Our simulations show that such measurements are perfectly feasible on MAGiC. Typically, such measurements for several hours will be sufficient for refining both nuclear and magnetic structures with 2-3 μ_B.

Structure determination on epitaxial films

Another very important science case is related to the magnetic structure in epitaxial films. Typical samples have a large surface area (5x5 mm^2) and 10 to 100 nm thickness. Here, the focusing device is not useful, as we want to benefit of the large sample surface. Today, experiments on thin films may extract valuable information from one to few reflections accessible. On MAGiC, a full data collection for structure determination on a 100nm thick film could be done in a few hours. Our simulation indicates the feasibility of studying monolayer films within few hours. It will be also an issue of background not only flux. Therefore substrate and nuclear signals will favorably be removed by the polarization analysis.

Studies of weak signals from thin films will fully benefit from the TOF-Laue method as it removes the issue of tedious alignments.

Structure determination with high Q-resolution on long period modulations

The ability for studying incommensurate magnetic ordering with long periodicity is an important feature of MAGiC. One of the most extreme cases is realized in the multiferroic $BiFeO_3$, which presents short lattice parameters (~4 Å in the pseudo-cubic setting), coupled to an incommensurate spiral magnetic order with a period of 640Å, corresponding to a multi-domain sample with propagation vector **k**=(0.0065 0 0)[66]. Such example is a perfect illustration of the high-resolution capabilities of MAGiC.

The simulation has been made on a $1mm^3$ $BiFeO_3$ sample using neutrons in the 3.7-5.4Å range and a 3 minutes counting time. To further improve the longitudinal resolution, the pulse length has been reduced to 500 μs. As seen from Fig.20, four satellites corresponding to **k**=(±0.0065 0 0) and **k**=(0 ±0.0065 0) in the scattering plane are observed with an excellent resolution. The obtained peak shapes are rather isotropic and Gaussian. At full pulse length, the low longitudinal resolution is hiding the splitting along the Q direction.

We may note that for the reference experiment on 6T2 at LLB (taking 12 hours), see Fig. 20, the special high transverse resolution has been obtained with the same collimation as used in the MAGiC simulation.

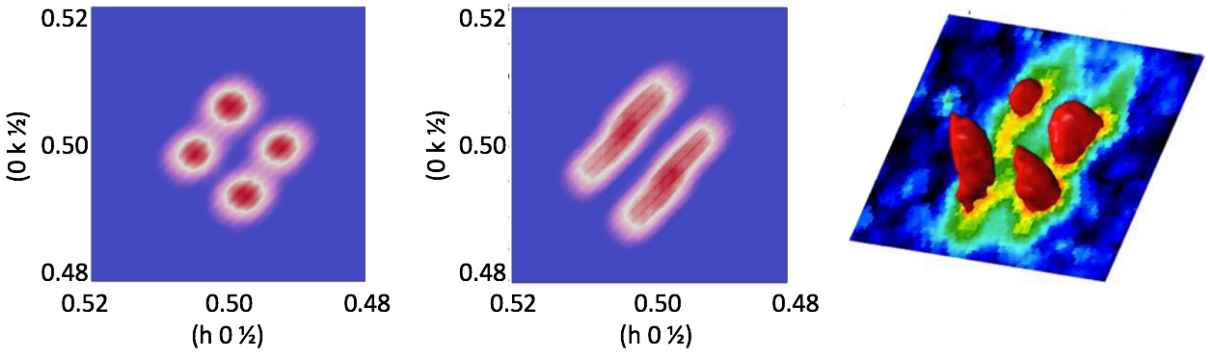

Figure 20: Diffraction pattern of the magnetic satellite reflections with 640Å periodicity in $BiFeO_3$.
Left: Simulation for MAGiC in high-resolution configuration (3.8 <λ< 5.5Å and 500 μs pulse length).
Center: The same simulation for MAGiC with full ESS pulse (like for NMX).
Right: Experimental results obtained on 6T2 at LLB.

Structure determination using polarized neutrons

We used the **molecular magnet** $Cu_2(NC_9H_{13})_4(N_3)_2(ClO4)_2$ [67] as a benchmark reference for a magnetic structure determination in the half-polarized setting, which measures the interference of nuclear and magnetic structure factors. The simulation gives a very challenging example from a today's perspective, because it contains only two unpaired electrons per formula unit consisting of 110 atoms including 52

[66] D. Lebeugle *et al.*, *Phys. Rev. Lett.* **100**, 227602 (2008)

[67] M. A. Aebersold et al, *JACS* **120**, 5238, (1998)

hydrogen ones. A relatively large number of reflections is required due to the low symmetry of the monoclinic structure P2 $_1$/c with a=12.39, b= 13.03, c=12.69 Å and γ=98.4°.

The experimental spin populations obtained after refinement are reported in Table 2 together with those obtained by density functional theory (DFT) calculations, predicting a magnetic moment of about 0.7 μ_B on the copper and ~0.1 μ_B on the nitrogen. We used the model predicted by DFT as an input of the scattering law for the McStas sample module, a sample size of 10 mm^3, and simulated an experiment with a full sample rotation and a total of 15 min beamtime. We obtained 600 (800) useful reflection, with R-1>**3σ,** for thermal (cold) setting of the instrument, reproducing successfully all features reported earlier in Ref. 62. (The reference work took two weeks of beamtime. Nowadays it could already be done within 2 days on VIP at LLB using a large 2D detector).

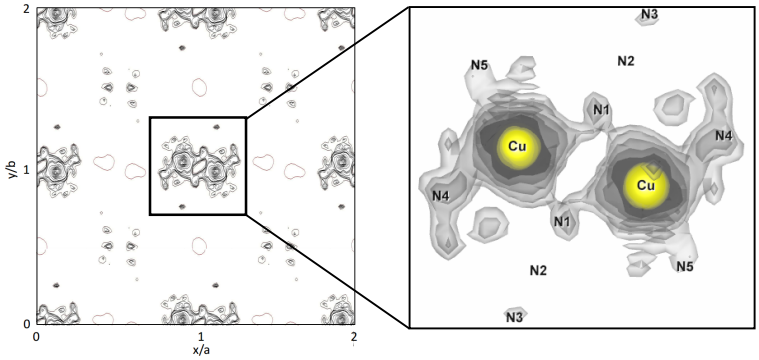

Figure 21: The spin density map of a molecular compound reconstructed by Maximum Entropy Method from MAGiC data, see text and Table.2..

Table 2: Calculated and refined spin population of Cu and N ions in the molecular compound $Cu_2(NC_9H_{13})_4(N_3)_2(ClO4)_2$

	DFT calculations (μ_B/ion)	MAGiC refinement (1**σ**)	Refinement Ref.[62]
Reflections used	NA	600	549
Cu	0.774	0.75 (1)	0.87(2)
N_1	0.069	0.08(1)	0.06(2)
N_2	-0.015	-0.014(10)	-0.04(2)
N_3	0.054	0.05 (2)	0.08(2)
N_4	0.067	0.07(1)	0.04(1)
N_5	0.048	0.06(2)	0.06(2)

Structure determination including XYZ polarization analysis

XYZ polarization analysis is the tool of choice to reveal weak magnetic signals hidden by nuclear contributions. The Varma state in superconductors is one of these cases; the weak current loop magnetic contribution appearing on top of nuclear reflections. Today, extracting the information on one single peak is a time consuming process, each point in temperature requiring several hours. More than a week is necessary to study the evolution versus temperature of one Bragg reflection, and no structure refinement of the current loop signal has ever been possible. The increased polarized flux of MAGiC, and the larger detector coverage will yield a 2 order of magnitude gain factor allowing such data collection in a reasonable amount of time.

Diffuse magnetic scattering including XYZ polarization analysis

To benchmark the capacity of MAGiC in diffuse scattering we have chosen the canonical spin ice $Ho_2Ti_2O_7$, which was measured on D7 (ILL) using a monochromatic beam and polarization analysis[68]. The relative instrument efficiencies can be essentially estimated by the flux ratios 10^3, although one could foresee possible flux gains of the D7 upgrade in the ILL endurance program. The diffuse scattering cross-section was simulated using the analytical model from Henley[69]. The simulations use the full pulse of polarized neutrons from the cold moderator ($2.0<\lambda<3.7$Å). We chose a small crystal of only 10 mm^3, which could provide also useful integrated Bragg intensities in the same measurement. 180 Laue patterns have been simulated, with 2° steps of sample rotations and 15 secs acquisition time per step. Within the total counting time of 45 min for a full rotation, one obtains ~10^3 counts near a diffuse peak in a dQ^3 element of 3×10^{-4} $Å^{-3}$, which is the estimated volume for a D7 detector cell. The simulated diffuse scattering is shown in Fig. 22.

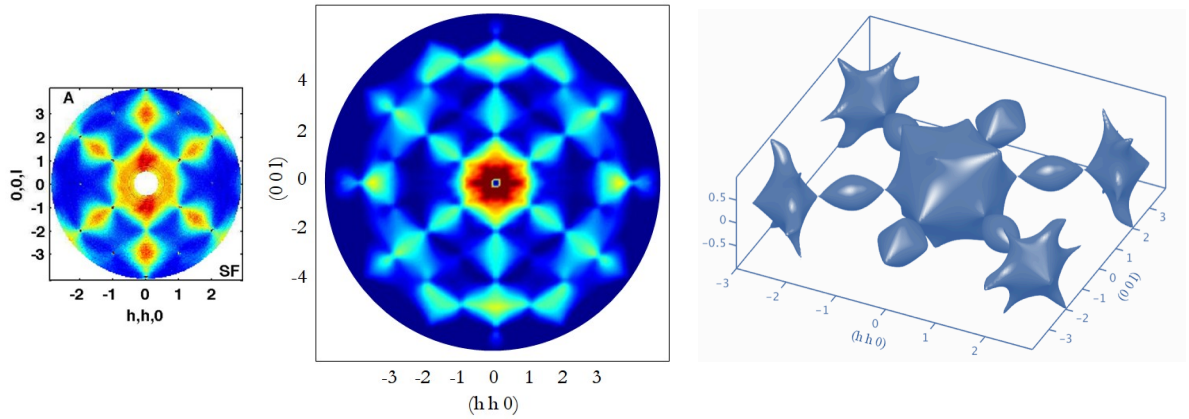

Figure 22: Spin ice diffuse scattering of $Ho_2Ti_2O_7$. *Left*: data from Ref.[67], D7 (λ=4.8Å) *Middle:* Simulation based on the model of Ref. [68], a 10mm^3 crystal on MAGiC (2.1-3.8 Å). *Right:* "Turtle and the stars", a section of the 3D iso-surface reconstruction from the MAGiC data without polarization analysis.

More features are revealed with extended Q-range (vertical $Q_z<1.6Å^{-1}$) and 3d-resolution ($dQ_z\sim0.02$ $Å^{-1}$), in particular, when using the large detector bank without polarization analysis. For illustration purpose, one of the equal intensity surfaces (iso-surface) obtained in the simulation is shown in Fig. 22. Note, such an option for a large position sensitive detector exists nowadays at the similar instrument DNS at MLZ[70]. It yields valuable 3D information about frustrated systems with local constraints.

A remark on performance

Performance/simulations show that rather short times for data collection are needed for many cases that are possible but challenging today. Such "future-standard" experiments need to assign relatively more time for sample handling, cooling, data visualization and inspection, and more. Very clearly, MAGiC will set new horizons for the "future-challenging" experiments, as can only be dreamed of for new science cases; cases that demand for flux, such as weakest moments, magnetic structure determination from synchrotron-size crystals and epitaxially grown systems.
There is a caveat. As pointed out by J. Carpenter, the triangle of unhappiness for neutron sources is made of (i) lack of brilliance, (ii) lack of neutrons and (iii) background, and relates more specifically to reactors,

[68] T. Fennell, *Magnetic Coulomb Phase in the Spin Ice $Ho_2Ti_2O_7$*, Science 326, 415-417 (2009)
[69] C. Henley, *The Coulomb phase in frustrated systems*, Ann. Rev. Condens Matter Phys. 1:179–210 (2010)
[70] http://www.mlz-garching.de/dns , polarized flux gain compared to DNS ~200

short-pulse and long-pulse spallation sources, respectively. Accordingly, ESS instruments need to be very concerned about background.

Background and signal-to-noise consideration

Bragg peaks are delta-functions in the 4 dimensional Q,ω-space and a TOF-Laue instrument like MAGiC resolves these peaks in 3D Q-space. Bragg diffraction is generally less sensitive to background compared to the dispersed 1D-Debye-Scherrer lines in powder diffraction or the case of 2D signals of magnon and phonon scattering. Hence, single crystal Bragg diffraction will be the ultimately remaining method in the extreme of smallest samples, where experiments will be limited by the achievable signal-to-noise ratio rather than by mere flux. Compared to powder diffraction and conventional Laue diffraction the signal-to-background should be cleaner by at least two orders of magnitude in TOF Laue diffraction, which also sets the different scale to observable signals and sample sizes.

The weak Bragg signal from the "**Varma state**", highlighted in the science case, is usually studied by triple-axis-spectrometers *and* polarization analysis.

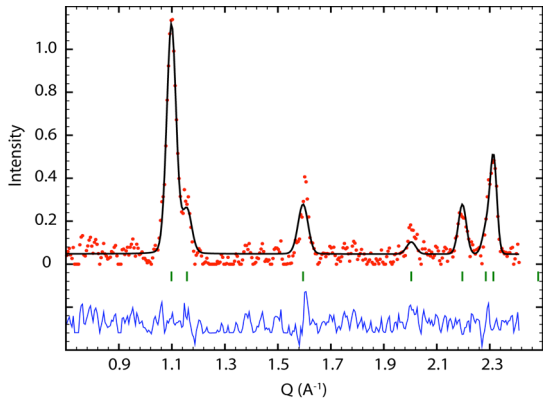

Figure 23: Elastic scattering from the S=1/2 kagome ferromagnet Hadyeeite **α**-$MgCu_3(OD)_6Cl_2$, measured on the TOF-spectrometer IN5 at ILL, yields a moment estimate of 0.2 μ_B. The unfavorable intrinsic background from the sample prevented an earlier solution on diffractometers.

Energy analysis for true elastic scattering is one important tool to further improve the signal-to-noise ratio. It is the reason, why TAS instruments are used for special diffraction applications[71], see example given in the Fig. 23.[72] One may note, the D10 diffractometer is often using energy analysis. Studies of weak magnetic moments may not be possible using energy integrating techniques such as neutron diffraction, when the inelastic fluctuations are much stronger than the weak elastic signals. Weak magnetic moments are of strong interest in quantum spin systems, where quantum fluctuations prevent full ordering of the moment, and heavy-fermion systems, and can be obtained from elastic neutron scattering with both, time-of-flight spectrometers and triple-axis spectrometers. The technique also helps when the sample environment is bulky, *i.e.* for pressure cells and high-field magnets. The option for energy analysis on MAGiC provides a few to about 1% resolution for the price of accordingly increased counting times.

Polarized neutrons and polarization analysis provide the other important tool, which enables to separate magnetic scattering from nuclear scattering, from spin-incoherent scattering and from essentially all scattering background as exemplified in Fig. 24. The background suppression relies on the degree of polarization and on the accuracy of the corrections from imperfect to perfect polarization. This is feasible typically at a 1 % level or better on the DNS instrument at MLZ as illustrated in the example below.
MAGiC will have even better quality in polarization. The possible improvement in signal-to-noise ratio is up to 3 orders of magnitude at the cost of only a factor 4 in loss of intensity, 2 by polarizing the beam and

[71] T. Taniguchi et al., Phys. Rev. B 87 (2013) 060408(R): See inset of Fig. 5.
Magnetic order of UPt_3 under uniaxial pressure, N. H. van Dijk et al. Phys. Rev. B 63 (2001) 104426.
Magnetic order of UPt_3 in high magnetic fields, N.H. van Dijk et al. Phys. Rev. B 58 (1998) 3186--3190

[72] D. Boldrin, B. Fåk, M. Enderle, S. Bieri, J. Ollivier, S. Rols, P. Manuel, A. S. Wills, http://arxiv.org/abs/1503.08023 , March 2015.

another factor 2 for analysis. A worst-case background is to have a weak magnetic Bragg peak on strong nuclear peak, it is THE CASE where polarization analysis is unique for background separation. MAGiC will offer polarization analysis only for the smaller 0.2 sr detector. The large detector accepts more background than a 1D detector or single counter. The difference of spin-up and -down intensities, which for example relates to field induced magnetic moments, however, will again be freed from background.

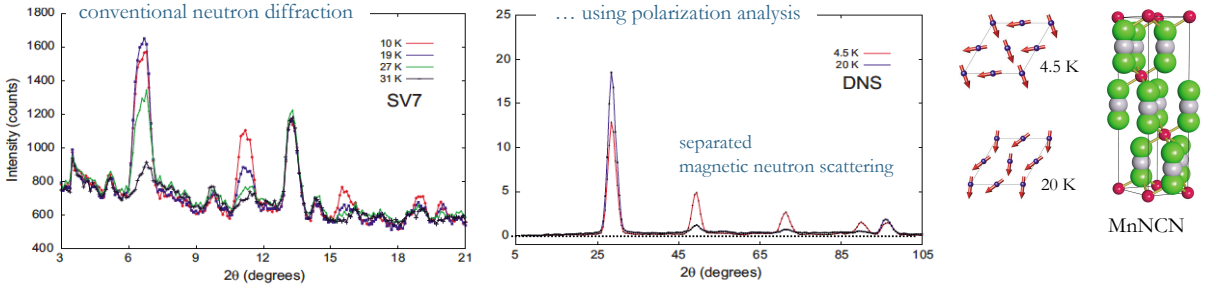

Figure 24 : Neutron powder diffraction with polarization analysis.[73]

Background will increase with the high unpolarized flux of up to 8×10^9 n/s/cm^2 and in view of current signal-to-noise limited experiments all measures ought to be considered to achieve a better signal-to-noise situation. Standard requirements are: evacuated primary flight path, Argon secondary flight path (enclosed volumes rather than flushing in view of activation[74]). The choices of Ar or the alternative He-filling will be evaluated in Phase1 with respect to radiation and safety aspects. Radial collimation (optional) and polarization analyzers act as collimators, slits limiting the beam size to what is strictly necessary.
There are also new opportunities for defusing mines in data fields: The proposed detector offers spatial 3D resolution and measures the trajectories of the ensemble averages, such it has an "in-built radial collimation". In radial projection towards the sample, Bragg signals from the sample remain point-like, resolution-limited, while Bragg signals from the environment will broaden with line-shape. Beyond this immediate gain, there is an obvious new opportunity (and a need for DMSC support) to develop algorithms for *a posteriori* data cleaning.

The ternary instrument: data analysis and software development, issues for DMSC

In the previous sections of the proposal, we presented full simulations of the instrument up to data acquisition. There is a series of challenges to assure that the high counting performance of MAGiC will also be transformed into successful publication output. Following acquisition, a complex data treatment has to be carried out in order to extract the physics from the experimental data. Most of this work has been presented[75] and incorporated in MANTID by the joint effort of IPNS, ISIS and SNS IT groups.

Currently MANTID is the platform of choice for TOF data treatment and is supported by all neutron facilities. In particular it is fully operational for single crystal structure refinement. However there is still work to be done to adapt MANTID to complex magnetism in single crystals and to include polarization in the software modules. This MANTID enhancement will be the result of a coordinated work between neutron facilities (ISIS, SNS, J-PARC, ILL, …), the ESS being part of it through the DMSC**.**

Software for fast 3D visualization is developing. One example[76], becoming available recently, creates a 3D transparent picture, which can be rotated in (user) real-time, providing the desirable fast view and possible first judgment of the data and its quality. The crystal orientation (UB-matrix) can be determined

[73] M. Krott et al., Phys. Rev. B 80, 024117 (2009).
[74] Ar-activation: 2.5kg Ar for 24h(1y) in ~$2x10^4$n/cm^2/s yields ≲ 250Bq (13kBq) after 1h
http://www.wise-uranium.org/rnac.html
[75] Arthur J. Schultz *et al*, Journal of Applied Crystallography 47, 915-921 (2014)
[76] Florian Rhiem, Master thesis, FH Aachen,
http://iffwww.iff.kfa-juelich.de/pub/doc/Masterarbeit_FlorianRhiem.pdf

by superimposing Bragg peaks sensitively by the user's eye. The code will be open source and compatible with MANTID for further analysis.

Additional information about the data treatment can be found in the Appendix B.

2.3.2. Comparison with other instruments

An important parameter for the capabilities of diffractometers is the available wavelength band, see Figure 25. Short-pulse spallation source – and hot source instruments offering shortest wavelengths are best suited for high-resolution crystallography and but also form-factor measurements. MAGiC covers a broad science spectrum in magnetism with offering neutrons with λ>0.6Å and benefits from the adaptable resolution and the ESS long pulse.
Gain factors need to be considered with care. A comparison is most clear by using specific cases as shown above in full experiment simulations or by comparison to an actual measurement (see TOPAZ example). The largest gains ~10^5 are obtained for the purpose of magnetic structure determination, comparing to a 4 circle- or single-counter diffractometer, where TOF Laue measures hundreds or thousands peaks simultaneously, without need for scanning and with even superior time-average brightness.
One may note, in opposite, if only the signal of a single peak matters, a TAS like instrument and MAGiC will be more competitive with respect to count rate and signal-to-noise ratio.

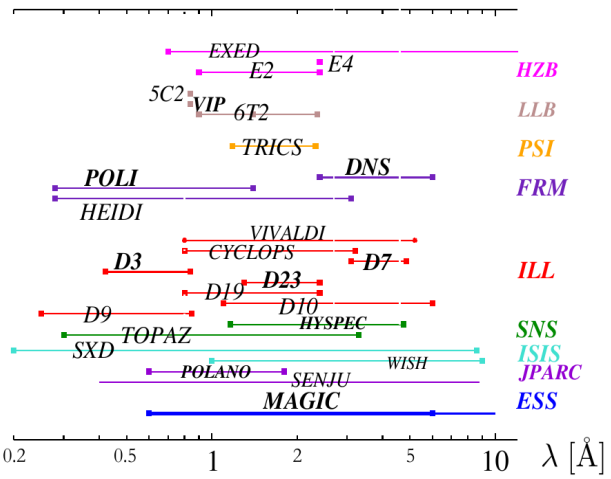

Figure 25: Neutron Instruments used for magnetic diffraction and available wavelengths.

For the following instrument comparisons, we assume that the interest is in measuring an appropriately extended range in Q-space, as needed for structure determination and diffuse magnetic scattering.
With respect to other instruments, see Figure 25, MAGiC offers by far the highest flux, most flexibility, high polarization, with dedication also in sample environment to needs of the magnetism community.

A more detailed instrument comparison is given in the Appendix C.

2.3.3. Uniqueness and integration in the ESS instrument suite

Among the accepted ESS instruments, NMX and DREAM are offering TOF-Laue techniques for studying single crystals.

NMX is a dedicated instrument for macromolecular crystallography, *i.e.* very large unit cells (lattice parameters >150 Å) and very small crystals. NMX uses only the cold moderator flux and is optimized for collecting Bragg intensities with very high transverse and lower Q resolution due to the lack of pulse shaping choppers. An important distinction of MAGiC is its polarized beam.
DREAM is optimized for powder diffraction with a bispectral larger wavelength band, however may serve similarly to WISH also for single crystal diffraction. It has nearly 2π sr detector coverage. The transverse Q-resolutions are comparable to MAGiC and the longitudinal resolution of DREAM optimized for powder diffraction is very flexible. Specialized sample environments on DREAM are well acceptable (magnets or high pressure cells) however, will reduce the usable detector coverage. An important distinction of MAGiC is its polarized beam.

The proposed instrument MAGiC is specifically optimized for the user community investigating magnetic phenomena in various experimental conditions. It will be designed to accommodate diverse sample environment, permanent magnetic fields, pulsed fields and others. Moreover, MAGiC offers a beam with high polarization and capabilities for polarization analysis as most important and unique feature. Energy analysis can be used to eliminate inelastic background and for quasi-elastic studies.

2.4. Upgrades

Pulsed high magnetic fields:
This is a very attractive option for the case of ultimate high fields, which we aim to realize as early as possible. We plan to develop in collaboration with the LNCMI Toulouse a **conical magnet** generating **60 T** horizontal field. The use of a split-coil generating vertical field has been also considered, however, such magnets offer a reduced duty cycle as well as a lower maximum magnetic field. The proposed device is based on a resistive coil design made of high tensile wires. The wiring is made over a stainless steel double cone ensuring vacuum and thermal insulation between the sample volume and the coil/LN_2 volume. The magnet design provides a conical aperture of 60° for the scattered beam and of 30° for the incident beam.

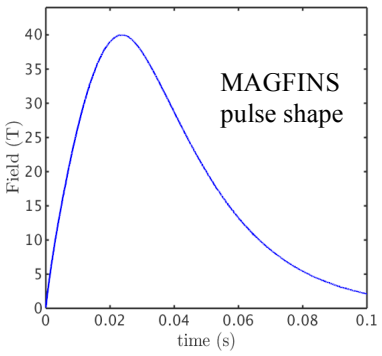

Figure 26: Pulsed magnetic field profile of the LNCMI 40T MAGFINS conical coil.

Using 3 MJ capacitor bank, such coil can achieve 60 T with full pulse width of 140 ms and 10 mn repetition rate. Operating the setup at 50T will limit the total energy to 2MJ and increase the repetition rate to 1 pulse per 6 mn. Repetition rates are mainly limited by the coil cryo-cooling by liquid nitrogen. The duration of maximum field (>90%) is above 20 ms. Magnetic pulses will be fired through fully optical thyristors and triggering system and can be synchronized with the ESS pulse and wavelength spectrum.

This design is currently under operation at the ILL. The IN22 magnet is achieving 40 T at 1.1 MJ. The last 10 years have witnessed a doubling in pulsed magnets capabilities on synchrotron/neutron sources. The maximum achievable field will certainly increase by design, wire optimization and cooling improvements over the next 10 years. Construction cost of the magnet itself is rather moderate (<500 k€). Most of the pulsed magnetic field setup cost lies in the capacitor bank (1.5 M€). Several instruments may want to share use and cost of such a setup, and efforts would be coordinated by the sample environment group.

Polarization by ^{3}He filter cells: ^{3}He filter cell is relatively inexpensive (100k€) and should be considered if ESS will be able to provide the resources for operation.

Increase of detection area/solid angle: For using a larger angle of detection in Laue diffraction one may further increase the detector area. There are two possible upgrade paths, first to replace optionally the detector bank with polarization analysis, and second to continuously increase the out-of plane coverage. The first case will add 1.5 M€ with a factor 2 performance gain, while excluding polarization analysis, the second case will add 1 M€ with 23% additional Q_z-space coverage.

2.5. Technical Maturity

The maturity of the main instrument components is discussed in further detail within the description of the components. Here we give only a brief summary.

Detector
The detector of our choice, meeting our requirements, is the Jalousie-type detector. This type of detector is currently under construction for the POWTEX instrument at MLZ and the same detector type is also considered for the DREAM instrument. For MAGiC there are less geometrical constraints for the detector. The 3m² large detector can be assembled in a modular structure based on a single unit module type. Prototypes of this module have been successfully tested (G. Modzel et al. *NIM* A **743**, 90-95 (2014)).

Solid-State Bender
Solid-state benders have been developed and tested in various neutron facilities. As an example, SNS made test on a polarizing solid-state bender yielding P>97% on a large wavelength range as expected from simulations. One of the major difficulties is the Bragg extinction of the bender, which strongly scatters specific wavelength. In the range of the cold moderator this is however less critical with only one peak around 5.2 Å. The Silicon absorption reduces the transmission by 10-20% and is taken into account in our simulations. While the performance of the solid-state bender appears to be superior to other alternatives, there is a lower risk by having the device movable and adjustable outside of the monolith.

Guide
A specific feature of the neutron guide will be the polarizing FeSi supermirror coating. The requested coating is within the current state of technology. McStas simulations showed that 80% of the total guide length can be coated with m=2. The remaining 20% are located in the first and last 10 m of both elliptical sections and on the forced reflecting side of the straight element. In this parts, an adaptative m-coating will be used with a mean value of $<m>$=3.5.

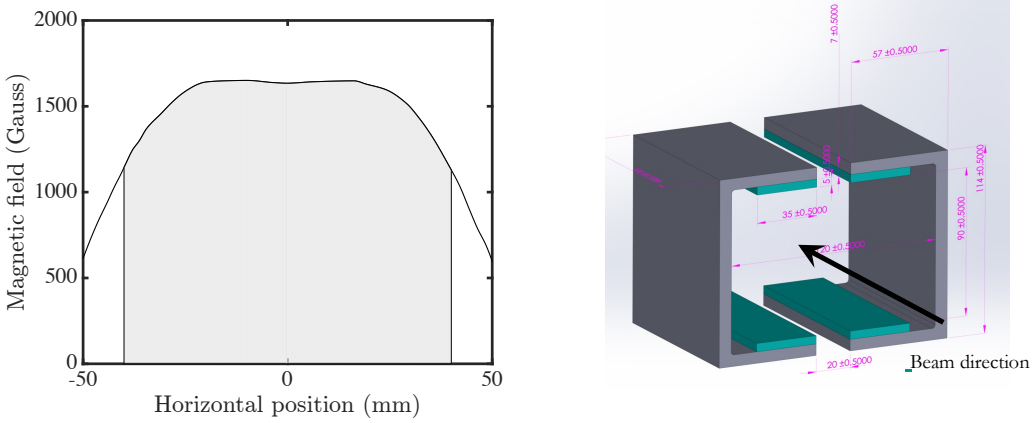

Figure 27: *Left*: Horizontal 1D cut of magnetic field distribution in the guide induced by 4 NdB permanent magnets. Shaded area corresponds to the inside of the guide. *Right*: Drawing of the magnet configuration simulated.

Permanent magnets with a yoke along the guide preserve its polarization and are available on request from neutron guide producers. The FeSi supermirrors as currently produced require at least 300 G to be sufficiently magnetized. The performance increases with field up to 1000 G. The latter is challenging, but our COMSOL simulation shows a 1150 G magnetic field on the guide wall using commercially available Nd permanent magnets with 0.5 T at surface. We have not yet investigated the required length of the polarizing guide, possibly, this can be only a small fraction of the total guide.
There is a save alternative with a non-polarizing guide.

Choppers
Choppers needs of MAGiC are covered by current existing technology with respect to disc diameters,

frequencies, bearings, and materials (either high strength Al alloys or carbon fibers are possible). The pulse shaping choppers are counter rotating and use magnetic bearings. The 14 Hz (SC) pulse selection chopper is less critical also with separation to the PSC. The Fermi choppers will use a Si-wafer slit package, which is a favorable more recent development (TOPAS at MLZ, new chopper for 4SEASONS at JPARC).

Superconducting magnet

A most recent survey with commercial suppliers (by ESS Scientific Activities Division) confirms that the currently available vertical split designs remain limited around 15 T. Development efforts focus on designs with an inner high-temperature superconducting coils set, combined with an outer coil-set based on NbSn-technology. Compromises with respect to homogeneity at the sample position and vertical apertures will allow a maximum magnetic field strength exceeding 20 T. We aim for the highest field available in time for MAGiC and CAMEA operation with a shared budget of 2 M€ for such a frontier cryomagnet.

Polarization analysis and cold polarizing extraction switch

The principle of polarizing solid state benders using Si-wafer stacks coated with FeSi supermirrors has been shown to be very efficient and superior to air-gap polarizers as well as cavities, as demonstrated with the polarizer used at the MIRA instrument at MLZ.

The solution proposed for MAGiC is a wide-angle super-mirror polarization analyzer in front of the detector to one side. In contrast to existing wide-angle super-mirror polarizers, those at DNS, D7 and HYSPEC, we plan to build this device with Si-wafer stacks with a FeSi coating. The principle is the same as for the incident polarizer. A prototype is currently planned in a joint project by PSI (experience by building the HYSPEC analyzer) and JNCS (experience by building the DNS analyzer). The HYSPEC analyzer can be considered for a fall-back option.

Flipper

The Mezei-type flipper provides most flexibility. It can be ramped precisely in time matching the coil current to the time dependence of the ESS pulse. The time-constant $\tau = L/R$ is short (inductance $L \sim$mH) and determined by resistivity of the power supply. The largest uncertainty in $\Delta\lambda/\lambda$ given at shortest wavelength 0.6 Å and full pulse still keeps the polarization up to 0.99. Such a device is currently used at the spin-echo instrument at SNS to obtain a pi/2 flip ramping in time for the whole wavelength spectrum. The (AFP) RF-flipper is a save alternative for a pi-flip.

Polarized neutrons and TOF Laue method

One may consider two typical modes of operation: (i) stepwise, with polarization changes for each step and data collection synchronized with the source pulse, (ii) continuous rotation, with polarization change after completing a rotation. One may note that the second approach is also feasible, because the TOF-Laue method will provide proper peak integration, and one does not need to rely on measuring flipping ratios only.

There will be resources from DMSC (not in instrument budget) of an instrument scientist for two years to support special software development for the instrument.

2.6. Costing

Detector and data acquisition: The detector technology is based on the POWTEX detector, which is currently under construction and which is further the detector proposed for the DREAM instrument. The design of MAGiC has the same requests in spatial resolution (4mm), pixel density and detection efficiency. The large detector will cover an area of ~3m^2, the smaller detector ~0.1m^2. The cost is estimated to 1.6M€ and 0.4M€ for the larger and the smaller detector, respectively.
Sum: **2 M€**

Neutron guide system: The costs for the 157m long guide, vacuum housing, support system, installation of the guide system amount to ~2.75 M€. Cost for the magnetic field is estimated to 200 k€. Costs for the vacuum pumps and vacuum control systems are estimated to 60k€. The optical component for the bi-spectral extraction in the solid-state bender version is estimated to 150k€. Sum: ~**3.2 M€**

Shielding: ~ 2 to 3 M€ (preliminary ESS estimate)

Polarization analyser: The cost estimate for this device has a relatively large uncertainty and is determined by the Si-wafers and sputtering: ~**2 M€**

Choppers: We estimate 0.5 M€ for the two pulse shaping chopper, 0.1 M€ for the 14Hz selection chopper, 0.15 M€ for the band control chopper, 0.4 M€ for the Fermi chopper system. Sum: ~**1.15 M€**

Magnets: high field 20T+ split coil superconducting magnet **1 M€**
(assuming 50% share with CAMEA)

Instrument infrastructure and specific support equipment: **0.5 M€**

Integrated design: The effort from the Lead Scientist and Engineer, as well as other scientists and engineers involved in the overall instrument design. (Staff) **1.7 M€**

Procurement, installation and commissioning: (Staff) **1.3 M€**

Systems Integration: Systems engineering to ensure compatibility between components and compliance with ESS standards. (Staff) **210 k€**

Total: ~ 15 – 16 M€

Upgrades

(1) 60 T pulsed magnetic field	+ 0.3 M€ magnet and cryogenics
	+ 1.5 M€ capacitor bank (share with pool or other instruments)
(2) ^{3}He-polarization analysis	+ 0.1 M€ (operational costs excluded)

Furthermore, one may consider spin and flipper modulation techniques (<0.1 M€ + PhD or post-doc) and a possible increase of detector area (up to 1.5 M€).

PROPOSAL HISTORY

New proposal:	Yes

Appendix A – Report on TOPAZ experience

To validate our simulations, we performed an experiment on TOPAZ at SNS. TOPAZ is a Laue-TOF single crystal diffractometer dedicated to crystal structure studies. It has large detection coverage on one of the most advanced spallation source in operation. In this respect, it is of interest to show the possibilities of this instrument type and to compare the performance of TOPAZ with MAGiC. One should note however, that TOPAZ is not particularly dedicated for science cases related to magnetism. It cannot cover the needs for low temperatures or high magnetic fields (Anger camera detectors) and does not offer polarized neutrons.

We performed a diffraction experiment on a $(La_xSr_{14-x})Cu_{24}O_{41}$ compound. In these composite compounds, two sub-lattices are coexisting, ladders and chains, with different c parameters. The orthorhombic unit cell is defined by a=13.2 Å, b=11.41 Å and c=3.9 Å for the ladders and c=2.75 Å for the chains. An effective large unit cell can be defined containing both the ladders and chains with c=27.5 Å. The large effective lattice parameters yield a huge number of attainable reflections with a wavelength range on TOPAZ from 0.4 Å to 3.6 Å. The sample volume used was of 1.5x2.5x2 mm^3 with a close to perfect rectangular shape. (Due to relatively small beam size (3x3 mm), samples bigger than 2 mm are not used on TOPAZ.)

Unfortunately, no magnetism study is currently possible on TOPAZ as it is not equipped with proper cryogenics yet. The minimum temperature achievable on sample using nitrogen flux is 90K. The advantage tough is that in this case there is no material in the beam neither in the incident nor in the scattered beam, which decreases enormously the background. TOPAZ is equipped with a kappa goniometer (with rotation angles ω, φ and χ=135°). Samples are glued on magnetic pins and centering of samples is made by in-situ video camera using piezzo-electric drives.

Data acquisition strategy is defined by the CrystalPlan software which maximize Q-space coverage and minimize the total number of angular positions for a desirable redundancy factor. 12 positions were required in our case with an hour counting time for each, with redundancy factor of about 3. Data set obtained at each position contained a list of about $3x10^7$ events and occupied ~300 Mb. A total of 600 peaks (>3σ) were typically found and indexed for each sample orientation. Once data acquisition is launched, a live access to data is available. One can visualize slices in Q-space, find Bragg spots, find the lattice parameters by FFT and refine the UB matrix. The full data reduction suite is based on the MANTID platform. Structure factors extraction from a data set is done during experiment with a typical delay of an hour from the time of the set acquisition, essentially due to rather complex binning procedure of raw data.

After the experiment SNS is giving a free remote access to its high performance computing possibility to users, but we have transferred raw data to Saclay in order to re-treat them. The treatment using MANTID was possible only on our dedicated high performance computer (>128GB of RAM and 48 logical cores), as the memory requirements for single crystal data reduction are quite high. The full data reduction process is now operational at the LLB on this computer, which allows to:

- Load one or all datasets (20s / dataset)
- Convert each dataset to instrument Q-space (40s / dataset)
- Apply absorption correction based on wavelength, sample shape, and composition. Detector efficiency is also corrected automatically (2 mn / dataset).
- Find all peaks in a given dataset using user-defined threshold (5s / 2000 peaks)
- Refine UB matrix based on the obtained peak list (2s). A few matching UB matrix are proposed to the user.
- Index peaks using the refined UB matrix (5s).

- Integrate peaks using one of the proposed algorithms (spherical, ellipsoidal, cylindrical). This part of the process is not yet optimized and takes ~40mn for 2000 peaks (per dataset in our case) on our dedicated computer.
- Export a list of hkl and associated intensities for data treatment.

The total processing time is currently close to an hour per dataset being comparable with the acquisition time. There is a lot of room for improvement on the integration algorithm as it is not parallelized and operates only on one core. Optimization of the software should reduce the total data treatment time down to a few minutes.

Preliminary crystal structure refinement using Amma(00γ) Super Space group has been made using JANA2006 which has been recently adapted for the output format of TOPAZ data. This was necessary to account for the wavelength dependence of extinction corrections occurring in Laue-TOF method. Final R-factors of 6.9% was achieved on main sub-lattices reflections after merging and 7.2% on first order satellites. Higher satellite orders (up to fourth) were extracted and refinement is still in progress.

This shows that TOPAZ, and other Laue-TOF instruments in general, are now extremely efficient for high-resolution crystal structure determination, and in some cases competitive with X-ray scattering instruments.

Remarks:
- The whole data reduction process is operational but not yet sufficiently user friendly. Participation of local contact in data treatment is still strictly mandatory.
- Data treatment on incommensurate structures is not available yet. This problem needs to be solved on MAGiC, which will regularly deal with incommensurate magnetic structures.

MAGiC simulation: we performed a simulation of the same experiment on MAGiC to confirm the validity of our estimated counting time. Based on SNS flux and repetition rate, we estimate a 60 gain factor for MAGiC in count rates. However, this huge gain factor has to be taken with caution due to other relevant parameters:
- TOPAZ wavelength range extends down to 0.4Å. The effective 3D Q-space covered by TOPAZ is more than 3 times higher than the one of MAGiC.
- Longitudinal resolution on TOPAZ is much better at short wavelength, allowing for studying compounds with larger unit cell without pulse shaping, while MAGIC in this case will have to be used in pulse shaping mode decreasing the usable flux.

Using structure factors of reflections observed on TOPAZ we have simulated a scattering pattern on MAGIC obtained by full sample rotation. We obtained similar statistics as on TOPAZ in 11 minutes within the Q-space accessible on MAGIC ($Q_{max}<20$ Å $^{-1}$) and poorer longitudinal resolution. This resolution was, however sufficient for the proper intensity integration with the lattice parameters of our sample. It corresponds to a 66 gain factor close to the expectation. This result validates the time estimates made in the proposal for the various examples.

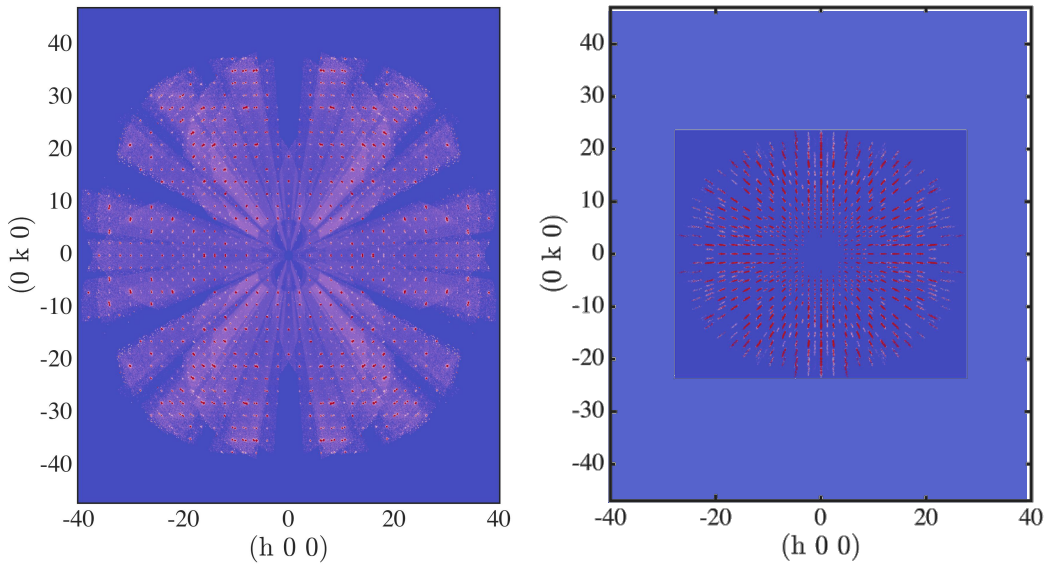

Fig. : *Left* : (hk0) diffraction pattern obtained on TOPAZ. *Right* : (hk0) diffraction pattern obtained in MAGiC simulation. TOPAZ pattern corresponds to a 12 hours acquisition time while MAGiC one corresponds to an 11 minutes one. Both patterns make use of the orthorhombic symmetries.

Appendix B – The ternary instrument

In the proposal, we present full simulations of MAGiC up to data acquisition. There is a series of challenges to assure that the high counting performance of MAGiC will also be transformed into successful publication output. Following acquisition, a complex data treatment has to be carried out in order to extract the physics from the experimental data. We present here a list of data manipulation and/or correction to execute. Most of this work has been presented[77] and incorporated in MANTID by the joint effort of IPNS, ISIS and SNS IT groups.

Data integration:
- The experiment can be made as a classical Laue-TOF mode or preferably, in a continuous rotation mode. In the latter case the instrument will operate as a multi-monochromatic instrument.
- The first operation is to convert the event data into the instrument Q-space. An adaptative mesh refinement is then performed, sorting density voxels and allowing fast and efficient peak search.
- A fast Fourier Transform algorithm is applied on the detected peaks in order to refine the orientation matrix (UB matrix). A list of matching unit cells is proposed to the scientist to convert the event data into the sample Q-space.
- Each of the detected peaks is integrated. Various algorithms, like spherical, ellipsoidal, cylindrical or 1D shape refinement, have been developed and recently incorporated in MANTID (ref 67). All of them are equally performing, the simplest one, spherical integration, being one of the fastest.
- A list of hkl is then generated with the corresponding structure factors, wavelength, and parameters necessary for extinction correction.

Data correction and analysis:
- Absorption routine is already integrated into MANTID and is well performing.
- Extinction and incident spectrum inhomogeneity: Bragg extinction effects from various materials in the incident beam path may affect the incident spectrum and need to be taken into account for the refinement based on (hkl, F, wavelength) sets. The wavelength dependence of extinction correction has been recently introduced in JANA2006 to deal with Laue-TOF data. Extinction is a known problem from the Laue-instruments (Vivaldi and Cyclops). The continuous rotation combined with the TOF-Laue mode of MAGiC will allow spotting any irregularities by too weak reflectivities in a λ-dependent Bragg-profile. Indeed, each Bragg-profile has to match the defined flux curve and each dip irregularity can be rejected.

Expected R-factors: Actual R-factors on TOPAZ at SNS are as low as 3 to 4% and comparable to best monochromatic instruments at reactor facilities. Based on the contributions of both SNS and ISIS to MANTiD and the strong involvement of DMSC at ESS, further prospects are very good. We are confident that such R-factor will be obtained on MAGiC.

There has been a lot of progress within the development of MANTiD. For Laue refinements, it still needs adaption to studies of incommensurate structures, which are particularly prominent in magnetism, and one may expect to see further efforts to make it faster and more user-friendly.
Software for fast 3D visualization is developing. One example[78] becoming available creates a 3D transparent picture, which can be rotated in (user) real-time, providing the desirable fast view and possible first judgment of the data and its quality. The crystal orientation (UB-matrix) can be determined by superimposing Bragg peaks sensitively by the user's eye. The code will be open source and compatible with MANTID for further analysis

[77] **Arthur J. Schultz *et al*, Journal of Applied Crystallography** 47**, 915-921 (2014)**
[78] Florian Rhiem, Master thesis, FH Aachen,
http://iffwww.iff.kfa-juelich.de/pub/doc/Masterarbeit_FlorianRhiem.pdf

Appendix C – MAGIC gains versus MAGIC challenges

Future trends in single crystal diffraction will be to more **complex** problems, more detailed information and the **smaller samples** that are common with **new materials**. The most important requirement is for **higher intensity**, since only then can statistics and resolution match the trend toward complexity, detail and new materials provided that the **background** and the **data treatment** are mastered. In diffraction, this means moving towards very **large 2D detectors** and **focusing neutron optics** in combination with flexible collimation devices easily adaptable to the sample size and requested divergence**.**

At present, reactor sources, with the ILL as a leading reactor, dominate the neutron single crystal (SC) diffraction. However, with the appearance of more powerful spallation sources, like ISIS T2, SNS, JPARC, the construction of the ESS and the expected shutdown of some reactors, the neutron landscape in Europe might change severely in the next five-ten years. Here we present our opinion how the construction of MAGIC will influence this landscape and what gains can be expected of its construction.

Only in Europe there are more than twenty single crystal (SC) diffractometers operating in Constant Wavelength (CW) mode on the reactors sources. As far as spallation sources are concerned two diffractometers based on Laue TOF method (SXD and WISH) work at ISIS and three (MANDI, TOPAZ and CORELLI) at the SNS. MAGIC will be primarily used as a Laue TOF instrument.
We shall try to estimate potential gains of MAGIC. With a focus on magnetic structure determination, this is an ideal winning case for MAGiC. One should be aware that for a different purpose, gain factors will be very different, particularly for parametric studies on a phase transitions measuring a single peak only.

Roughly speaking the performance of a diffractometer is linearly scaling with the source **brilliance**, brilliance transfer of its **neutron optics** elements ((i. e. **guide** in the case of TOF diffractometer and **monochromator** in the constant wavelength one) and **detector coverage**.
The highest currently existing time-average source **brilliance** is provided by the high flux reactor at the ILL, which possesses 5 constant wavelength (CW) diffractometers (D3, D9, D10, D23, D19) and two Laue ones (LADI-III, CYCLOPS). The FRMII has a similar flux and 3 CW diffractometers (HEIDI, RESI, POLI). The ORPHEE reactor with four times lower brilliance has 3 instruments (5C1, 5C2, 6T2), four CW diffractometers operate in Berlin (E2, E4, E5, V1) and one (TRICS) in PSI. All of the above CW diffractometer are using a thermal or hot source.

Among the thermal instruments, many of these use the standard wavelength λ=2.4Å operating with pyrolytic Graphite (PG002) and PG filter to avoid high order contamination. (Note, for MAGIC this corresponds to the peak of the cold moderator spectrum.) Their high intensity comes from the the high PG reflectivity of ~80% at this wavelength. The highest intensity is obtained when the instrument is mounted directly on the beam tube (D19, 6T2, E4), as in this case **wavelength focusing** in horizontal direction and **vertical focusing** (VF) are used. These instruments are frequently used for the magnetic structure determination, however, their maximum scattering vector accessible is quite low, $Q_{max} = 4\pi \sin\theta/\lambda < 4\text{-}5$ Å^{-1} , insufficient for the crystal structure solution. Presently the crystal structure is determined prior to the magnetic structure determination using X-rays or neutron diffractometers.

Table 1. Diffractometers, λ =2.4Å. All use PG002, (*) denotes vertical focusing.

	<Flux> n/cm^2/sec	Detector solid angle	field H
D19*	10^8	1.1 sr	
6T2*	3~10^7	0.18 sr	7.8 T
D23	7x10^6	SC	10 T, 12 T
D10	5x10^6	0.007 sr	10 T
E2	2x10^6	4x0.12 sr	
E4*	8x10^6	0.11 sr	16 T
TRICS*	10^6	0.11 sr	4 T

As far as neutron diffraction is concerned, high-resolution crystal structure determination is best achieved on thermal or **hot** neutron diffractometers like D9, HEIDI, 5C2 with $Q_{max} \leq 25$ Å^{-1} or Laue TOF machines SXD, TOPAZ. MAGIC provides a very high flux of both thermal neutrons and cold neutrons and can be used for the determination of magnetic and crystal structures, consecutively. Most important is that it will be done on the same sample and in the same experimental conditions, This is of particular importance for the studies of materials with spin lattice coupling under external magnetic, electric fields, high pressures and ultra low temperatures.

Table 2 summarizes technical parameters of major currently existing **hot** and **thermal instruments**. As seen from the table they have lower flux compared to **cold** instruments, however, much bigger reciprocal space coverage ($Q_{max} \leq 25$ Å^{-1}).

Table 2. Diffractometers 0.3< λ <2.4 Å, (VF vertical focusing, SC single counter)

	λ	Beam	Mono	<Flux> n/cm^2/sec	Detector Solid angle	H
D19	0.8 –2.4 Å	Thermal source	Ge, Cu	10^7 ...10^8	1.1 sr	
D9	0.3 - 0.85Å	Hot source	Cu(311)	6 x 10^6	0.007 sr	10 T
5C2	0.84 Å	Hot source	VF Cu(220)	5 x 10^6	SC	
6T2	0.9 Å	Thermal source	VF Cu(220)	3 x 10^6	0.18 sr / SC	7.5 T
D23	1.3 Å	Thermal Guide	Cu	4 x 10^6	SC	10 T, 15 T
HEIDI	1.17 Å 0.84 Å 0.55 Å	Hot source	VF Cu Ge	1.1 x 10^7 5.4 x 10^6 2 x 10^6	SC	6 T
D10	1 – 2 Å	Thermal Guide	Cu	2x10^6	0.007 sr	10 T

Parameters for polarized neutron diffractometers are summarized in Table 3. Polarization is obtained either by a Heussler polarizing monochromator or with supermirror (SM) bender in combination with PG

monochromator, with a typical brilliance transfer of 30-40 % of the useful spin component. The instruments D7 and DNS are applied for diffuse scattering rather than quantitative Bragg diffraction.

Table 3. Polarized Neutron Diffractometers

	λ	Beam	Mono-chromator	<Flux> n/cm^2/sec	Detector Solid angle	Polarization
D3 PA possible	0.42 - 0.84Å	Hot Beam	CuMnAl	$10^6 - 10^7$	SC	95%
D7 PA possible	3.1 Å 4.85 Å	Guide	3xPG SM	10^6 $2x10^6$	0.4 sr 0.4 sr	95% 95%
DNS PA possible	2.4- 6 Å	Guide	2xPG SM	$5x10^6$–10^7	3 sr 0.1 sr	- 95%
D23	1.3 Å	Guide	CuMnAl	$2x10^6$	SC	95%
VIP(5C1)	0.84 Å	Hot Beam	CuMnAl	$2x10^6$	0.6 sr	91%
6T2	1.4 Å	Therma l Beam	VF PG+SM	$8x10^6$	0.18 sr or SC	98%

MAGIC belongs to the group of Laue TOF diffractometers listed in Table 4, in which a classical Laue instrument CYCLOPS at the ILL has been added for completeness. At present, instruments of this type, like SXD and TOPAZ are dedicated to crystal structure studies, SXD also for (non-magnetic) diffuse scattering at high Q. They have a larger coverage in Q space ($Q_{max} \leq 25$ Å $^{-1}$) and higher TOF resolution than MAGIC, together with WISH they are currently best suited to benchmark the MAGIC performance.

Table 4. Laue Diffractometers

	λ	Beam	<Flux> n/cm^2·sec	Detector coverage	Polarization
SXD (TOF-Laue)	0.2- 8.6 Å	Guide	$6x10^6$	6,28 sr	
CYCLOPS (Laue)	0.8 - 3.2 Å	Guide	~10^8	~6 sr	
TOPAZ (TOF-Laue)	0.3 - 3.3 Å	S guide	~10^8	2.8 sr	
WISH (TOF-Laue)	1- 9 Å	Elliptic Guide	~10^8	1.55 sr	
MAGIC (TOF-Laue)	0.6 -2.4 Å 2 -3.7 Å 3.7 -5.4Å	Elliptic Guide	$1.1x10^9$ (+-0.3°) $4.3x10^9$ (+-0.5°) $2.2x10^9$ (+-0.5°)	~2.9 sr	96% 99% 99%

For a comparison of the TOF-Laue diffractometer MAGIC with conventional CW diffractometers, we may consider MAGIC as a multi-wavelength instrument. With a time-resolution of 2.86ms in a TOF-frame of 1/14Hz=71ms, the natural resolution of the ESS pulse yields 25 distinct wavelength bands. For better comparisons to the CW instruments we assume the TOF-Laue diffractometer operating similarly in a continuous /or stepwise rotation mode. (Actually, continuous rotation will be the best way of operation.)

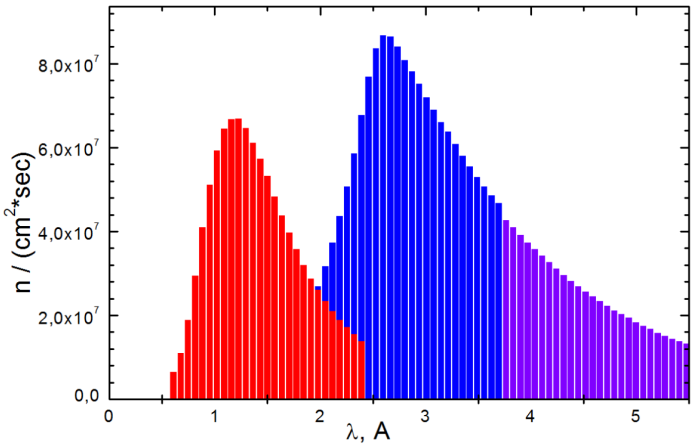

Fig. 1. Time of flight flux distribution at sample position in 3 histograms of 25 wavelength bands with a wavelength bandwidth δλ =0.069Å corresponding to a δt=2.86 msec.

The wavelength resolutions δλ/λ for the TOF-Laue instruments are determined by the primary flight path from source to sample and the pulse width. The pulse width at short pulse spallation instruments is given by the moderator characteristics. In case of MAGIC, we use pulse-shaping choppers to obtain flexible resolution with pulses from 200 μs to up to the natural pulse width of 2.86 ms.

	L	Δt	δλ/λ at 1Å
TOPAZ	18m	30μs	0.006
SXD	8.3m	~10μs	0.005
WISH	40m	100us - 150 μs	0.01 to 0.015
MAGiC	165m	200μs - 2.86 ms	0.005 to 0.07

Our MCSTAS simulations show that the full pulse resolution for cold neutrons (> 2.0 Å) is perfectly suitable for the investigations of magnetic structures with periods up to < 50 Å. In the extreme cases, like $BiFeO_3$ with periods above 500 Å, much better TOF resolution is needed, MAGIC can provide flexible pulse shaping and very tight angular collimation ±0.1°. This case is illustrated by a MCSTAS simulation in the main proposal.
The time-resolution can be matched to other TOF Laue instruments. A detailed comparison is shown for TOPAZ including a crystal structure study. For hot neutrons and smaller wavelength <0.6Å, the brilliance and time/wavelength-resolution of diffractometers at short-pulse spallation sources would be superior. Here, MAGiC does not attempt to compete and it would not be able to outperform TOPAZ or SXD.

The large **Detector coverage of TOF Laue instruments is** one of the most important gain factors, while the majority of existing CW instruments still operates in single counter mode. To illustrate the gains due to area detectors one can use the following example. For a crystal with lattice parameters ***a,b,c***~ 5 Å one has access to 250 reflections (with indices h,k,l<4) on a CW diffractometer with λ =2.4 Å (ratio a / λ = 2) . With 1 second exposition time per step, 30 steps and time losses due to angular displacements it

takes more than one minute of measurement per hkl, so the experiment will take more than 4 hours. (We note that in reality only 400-600 hkl per day are measured in average on current CW diffractometers.). If the lattice parameters are doubled, ***a,b,c*** ~ 10 Å, the number of reflection to measure will be increased by a factor of 8. Being proportional to $(a / \lambda)^3$, this gives 2000 reflection. We have to stress here that with λ =2.4 Å, we are still at the lowest acceptable limit Q_{max} = 4 $Å^{-1}$ for crystal structure determination. If the experiment is performed with thermal neutrons λ =1 Å (a / λ = 10) one in principle has an access to ~30 000 *hkl* reflections. Fortunately, for highly symmetric crystals, this number can be divided by the number of unique sets (varying from 2 to 48), but for low symmetric structures a single counter experimental procedure becomes totally prohibitive. In contrast, an area detector will allow getting the same information in one hour by recording 3600 data sets with steps of 0.1° and 1 second exposition time. The gain factor due to an area detector, being strongly dependent on the a / λ ratio, will vary for each experimental case. It is well known, however, that in extreme cases of a / λ ~100 which occur regularly in bio-crystallography the gain factors due to area detectors attain very high numbers (see NMX case).

Currently, the requests for crystal sizes are very different with respect to Bragg diffraction, discussed above, and diffuse scattering from single crystals. Sample sizes for Bragg diffraction are typically less than about $(3mm)^3$, and preferably studied with shorter wavelength in view of extinction effects. For diffuse magnetic scattering, extinction is negligible and crystal sizes are preferably large taking into consideration the weakness of diffuse signal. The two dedicated instruments DNS at MLZ and D7 at ILL routinely use polarized neutron and polarization analysis with larger detection area.
With MAGiC the situation is going to change. The large gain in cold flux will make it possible to measure much smaller samples, and enable to **measure Bragg and diffuse intensities simultaneously**. In addition to the flux gain, the possibility of shifting the wavelength spectrum to shorter wavelength for Bragg diffraction is important. The peak flux distribution of the cold ESS moderator perfectly matches the requests for combined Bragg and diffuse scattering measurements. The new concept of polarizing supermirrors made of Si-wafer coated with FeSi is able to provide high polarization efficiency for wavelengths λ > 2 Å, and with homogeneous response in transmission and polarization.

DNS is an instrument for diffuse neutron scattering using a multi-detector and polarization analysis for cold monochromatic neutrons within2.4Å<λ<6.2Å. The polarized flux is depending on wavelength and it attains up to ~10^7 n/s/cm^2. The incoming beam divergence at sample is 2° (horizontal) x 3°(vertical). The accepted divergence is 2°(horizontal) x 7°(vertical). The detector area is 0.1 sr with PA and 3 sr without PA.

D7 is using similarly to DNS cold monochromatic neutrons of fixed wavelengths λ=3.1Å, 4.8Å, or 5.7Å. The highest polarized flux is 2x10^6 n/s/cm^2. One may note that large gains are expected with an upgrade of the neutron guide system. The incoming beam divergence at sample is 2°(horizontal) x 3°(vertical). The accepted divergence is 2°(horizontal) x 7°(vertical). The detector area is 0.4 sr with PA.

Comparisons for the polarization analysis set-up:
For MAGiC, using polarized neutrons from the cold moderator with a wavelength-band of2.0Å<λ<3.7Å, the average flux will be 4.3 × 10^9 n/cm^2·sec, with 0.2 sr solid angle for PA.
Note that the incoming beam divergence of MAGIC is better defined, <± 0.5° horizontal and vertical. However, we have to compare for different wavelengths at the absolute resolution in Q-space. Approximately, for the considered band of shorter wavelengths, centered at 2.8Å, comparing to the monochromatic instruments at 4.8Å, there is a loss in Q-space density of $(2./4.8)^3$~1/5 and that roughly compensates the better divergence definition, arriving at similar Q-resolution, however, with a 5 times larger Q-space in this comparison.

Furthermore, the resolution of the MAGiC detector is higher as it is appropriately adapted for the cases of both peak- and integrated Bragg intensities. However, in typical cases, it is sufficient to measure only ratios of peak intensities with XYZ polarizations (see CRYOPAD or MUPAD), which can be refined using various models.
With the position sensitive detector and polarization analysis, MAGiC will also be able to resolve diffuse scattering with 3D Q-space resolution, however, limited by the detector height near to the horizontal scattering plane.

Comparisons for the half-polarized set-up:
With the large position sensitive detector, similar to an option at DNS, MAGiC will also be able to resolve Bragg and diffuse scattering in large 3D Q-space in unpolarized or half-polarized mode. With higher flux and better divergence, MAGiC will offer a much larger Q-range, with λ_{min}=0.6Å (MAGIC) and 2.4Å (DNS).